SOIL EROSION PREDICTION USING MODIFIED UNIVERSAL SOIL LOSS EQUATION (MUSLE) IN TUGEN HILLS, BARINGO, KENYA

BY

ATHANUS KOMEN CHESIRE

A THESIS SUBMITTED IN PARTIAL FULFILMENT OF THE REQUIREMENTS FOR THE AWARD OF DEGREE OF MASTER OF SCIENCE IN AGRICULTURAL & BIOSYSTEMS ENGINEERING,

DEPARTMENT OF AGRICULTURAL & BIOSYSTEMS ENGINEERING,

UNIVERSITY OF ELDORET, KENYA.

OCTOBER, 2022

DECLARATION

DECLARATION BY THE CANDIDATE

This research thesis is my original work and has not been submitted for any academic award in any institution; or in any format without prior written permission from the author and/or University of Eldoret.

CHESIRE K. ATHANUS

_____ _____

(PG/ABE/008/14) **DATE**

DECLARATION BY SUPERVISORS

This thesis has been submitted for examination with our approval as university supervisors.

_____ _____

PROF. WILSON NG'ETICH, PHD. **DATE**
SCHOOL OF AGRICULTURE & BIOTECHNOLOGY
UNIVERSITY OF ELDORET, KENYA

_____ _____

DR. JULIUS. K. KOLLONGEI, PHD. **DATE**
SCHOOL OF ENGINEERING,
UNIVERSITY OF ELDORET, KENYA

DEDICATION

I dedicate this thesis to my wife, Winnie and children Angela and Enock. God bless you.

ABSTRACT

Soil erosion by water is one of the primary causes of land degradation and occurs throughout the world. Soil erosion is contributing negatively to the already declining agricultural productivity thereby negatively influencing people's livelihoods and economic empowerment. Therefore, there is need to understand erosion processes, quantify sediment yield, identify and rank critical sources on spatial domain of sediment. This will help in formulation of prioritized catchment conservation strategies. This study focused on estimation of sediment yield from Tugen Hills particularly Saimo catchment in Baringo County using Modified Universal Soil Loss Equation (MUSLE) model with a view to develop an understanding of inter-relationships between soil erosion and sediment yield. The input model parameters of runoff volume (Q) and peak flow rate (q_p) were determined from runoff plots of dimensions 4.8m by 2m set up in the catchment with average slope of 2%. Soil erodibility factor (K) was calculated mathematically based on soil samples collected. Cover management (C) was obtained by percentage cover and support practice (P) factor was determined through observation and use of conversion table. Apart from determination of model parameters, the study calibrated and validated MUSLE for use in future studies within Saimo catchment and other catchments with similar characteristics. The mean bulk densities for top soil and bottom soil are 1.05g/cm^2 and 1.07 g/cm^3. The total value for fine sand and silt gives 37.1%. The saturated hydraulic conductivity varied from 8.0 µm/s to 41.3 µm/s with a mean value of 24.1 µm/s. There were only two classes high and moderately high translating to code 2 and 3, respectively. The analysis of variance (ANOVA) of the observed data showed that rainfall intensity affected the sediment yield production in the runoff plots and that there was no evidence to suggest that the soil homogeneity in the runoff plots affected the sediment yields. The observed and simulated MUSLE model values for calibration were PBIAS (0.83), R^2 (0.75), r (0.87) and KGE (-0.20) and those for validation were NSE (0.96), PBIAS (-0.44), R^2 (0.60), r (0.78) and KGE (0.46). Hence it can be concluded that the MUSLE model can be used successfully as an effective tool in soil conservation management. Future work for several seasons is however needed in order to capture different slopes and the varying climatic conditions for the model to be robust and to be used widely.

TABLE OF CONTENTS

LIST OF TABLES

LIST OF FIGURES

LIST OF ABBREVIATIONS

C	Cover management factor;
DAP	Diammonium Phosphate
Ha	Hectare
IE	Information Entropy
K	Soil erodibility factor;
Kg	Kilograms
LS	Slope length and steepness factor;
P	Support practice factor.
PSD	Particle Size Distribution
Q	Volume of runoff (m^3)
Q_P	Peak flow rate (m^3/s)
SDR	Sediment Delivery Ratio
Sy	Sediment yield (tons)

ACKNOWLEDGEMENT

I would like to acknowledge most sincerely the support of my supervisors Prof. Wilson Ng'etich and Dr. Julius. K. Kollongei for their continued guidance, suggestions and encouragement while developing, executing and writing my thesis. Much thanks go to my fellow students for their encouragement and support during my studies at University of Eldoret.

CHAPTER ONE

INTRODUCTION

1.1 Background Information

Soil erosion is defined as the process of soil components being separated and moved by erosive pressures (Ravi *et al*., 2010). It is a natural process that involves the entrainment and movement of soil components across a surface. It is the most widespread and severe kind of soil degradation, and as a result, it has a significant impact on agricultural land usage's long-term sustainability.

Sustainable development goal number 15 of the united nations advocates for the protection, restoration and promotion of sustainable use of terrestrial ecosystems with a view of reversing land degradation and loss of biodiversity. The recommendations made at the end of this study will form part of critical approaches that can be employed in addressing issues of land degradation question.

Wind and water are the two primary erosive factors on the soil. Water-energy erosion occurs when water falls on the ground, detach soil and flows across it, but strong winds can blow fragile soils away from flat or steep terrain. Water erosion naturally occurs as a result of the geological development of the land or as a result of man's interaction with nature (Balasubramanian, 2017).

Natural soil erosion has a small negative environmental impact. This can be found in natural waterways where there has been little human involvement. There is a delicate balance in such watersheds between sediment intake from upland areas and the ability of streams to transport those materials downstream (Al-Smadi, 2007).

Among other things, soil erosion causes nutrient loss, degraded land and agricultural yields, and lower soil productivity. Erosion transports fertilizers, pesticides, and other

dangerous farm chemicals into rivers, streams, and groundwater supplies, making erosion control critical to human survival (Carvalho, 2017).

Because of its extent, volume, velocity, and complex processes, accelerated soil erosion is a severe problem all over the world, with enormous economic and environmental consequences (Lal, 2017). Soil erosion occurs when land surfaces are damaged by a range of human-caused activities, such as agriculture. Soil erosion occurs more quickly in cultivated lands than in uncultivated ones. Cultivated areas operate as a conduit for transmitting nutrients, particularly phosphorus mixed with sediment particles into river systems hence soil erosion can be a severe environmental hazard (Ouyang and Bartholic 1997).

There are numerous methods for predicting water-induced soil erosion. Previous studies reveal numerous primary factors of soil erosion using data from about 8,000 communities in 36 locations across 21 states in the United States (Kouli *et al*., 2009). From their studies, they established the Universal Soil Loss Equation (USLE) to quantify soil loss by water. The long-term average yearly rate of erosion on a field slope is calculated using rainfall patterns, soil type, topography, crop system, and management approaches (Kouli *et al*., 2009).

The USLE model has been improved by gathering more data and incorporating recent research findings, and a modified version of this model (MUSLE) has increased its ability to predict water-borne soil erosion by combining new knowledge collected from more than 40 decades of studies (Chuenchum. *et al.,* 2019). Farming and tillage, road and building construction, forest logging, urban development, mining, and grazing are all examples of human activities that contribute to soil erosion. According

to estimates, moderate to severe erosion affects more than 80 % of the world's cropland (Ritchie *et al*., 2003).

Soil degradation is a huge global challenge because it causes the loss of both applied and natural nutrient status, as well as topsoil removal (Chalise *et al*., 2020). Previous studies reveal that soil erosion is responsible for more than 80 percent of the world soil degradation, with the bulk occurring since Second World War (WWII), culminating into about 17 percent loss in crop productivity (Rushema *et al*., 2020). Also, it is estimated that 35 percent of agricultural land in Asia, 45 percent in South America, 65 percent in Africa, and 74 percent in Central America is degraded (Scherr 2003).

Further research reveal that about 75 billion tonnes of soil are lost from agricultural lands worldwide every subsequent year resulting in an average financial loss of over $390 billion every year (Borrelli *et al.*, 2017). In Kenya, it is estimated that 30% of arable land is degraded (Bai, Z. G. and Dent, D. L., 2006)

Each year, around five mega grams per hectare (5 Mg ha^{-1}) of arable topsoil is lost to Africa's lakes and oceans (Angima *et al*, 2003). The restoration of croplands has resulted in increased agricultural yield per unit area and greater production expenses. High and rapid population increase, as well as inequities in the farm allocation resources are to blame, leading to inadequate management and over-exploitation (Nwokoro and Chima, 2017).

Human settlement, decreasing forest cover, and intense unregulated agriculture pose a threat to the future livelihoods of human and livestock in Tugen hills, Baringo County. The increase in human population has resulted in intense cultivation of steep slopes for agricultural output. As a result, the watershed has been stripped of native

vegetation, is intensely cultivated, and suffers from soil erosion, low infiltration capacity, decreased soil fertility, increased sedimentation of rivers, and high rates of surface runoff water (Wamithi, 2018).

The purpose of this study is to carry out soil erosion prediction using the modified Universal Soil Loss Equation (MUSLE) in Tugen Hills, Baringo County.

1.2 Statement of the problem

The cost of soil erosion in Africa is estimated to be $26 billion per year in lost productivity from the continent's productive soils. This crucial land management issue is undermining agricultural land productivity in the tropical Sub-Saharan Africa (Lal, 2017). In Kenya, between the year 2001 to 2009, an estimate of $1.3 billion per year is lost due to degraded agricultural lands (Mulinge *et al.,* 2016)F. Soil erosion is frequent in Tugen Hills, because of steep slopes with erodible soils and inadequate land management techniques (Odada, 2006, Johansson *et al.*, 2002). Soil erosion leads to; loss of planted seeds and seedlings, loss of topsoil which is always rich in plant nutrients and exposes subsoil which has poor physical and chemical properties, high runoff rates thereby accelerated loss of water and nutrients which would otherwise be used by plants. The degraded soils end up in the lower river basin, as well as in Lake Baringo to the East and Lake Kamnarok to the Northwest. However, information on quantification and prediction of the soil erosion in Saimo catchment is scanty.

1.3 Objectives

1.3.1 Overall Objective

The overall objective of the study was to estimate sediment yield from Saimo catchment in Tugen Hills, Baringo County, under different scenarios of land use and support practices.

1.3.2 Specific Objectives

The specific objectives of the study were to;

1. Determine soil erodibility, slope length and steepness, cover management and support practice factors to be used in Modified Universal Soil Loss Equation (MUSLE) model.

2. Calibrate and validate MUSLE model for surface runoff and sediment yield against field data.

3. Simulate sediment yield from Saimo catchment under different scenarios of cover management (C-factor) and support practices (P-factor).

1.4 Research Questions

1. How can the soil erodibility, slope length, steepness and cover management factors be determined for MUSLE model?

2. How well can the MUSLE model be calibrated and validated for surface runoff and sediment yield against field data?

3. How well does MUSLE model predict site specific surface runoff, sediment yield?

1.5 Hypothesis

The premise of this research is that MUSLE model is an effective tool in soil conservation management and that ANOVA of the observed data can be used to explain the impacts of rainfall intensity on sediment yield production in runoff plots.

Null hypothesis, $H0_1: \mu_{Treatment1} = \mu_{Treatment2} = \mu_{Treatment3} = \mu_{Treatment4} = 0$

$H0_1: \mu_{Block1} = \mu_{Block2} = \mu_{Block3} = 0$

- The rainfall intensity in the runoff plots within the Tugen hills do produce the same sediment yields during a rainfall event i.e., do have the same population means.

- The soils in the runoff plots (Blocks) are homogenous i.e., the physical and chemical properties that includes bulk density, soil texture, percent Organic Matter (% OM) and percent Organic Carbon (% OC) do not play significant role in sediment yield production in Tugen hills.

Alternative hypothesis, $H0_2$: $\mu_{Treatment1} \neq \mu_{Treatment2} \neq \mu_{Treatment3} \neq \mu_{Treatment4} \neq 0$

$$H0_2: \mu_{Block1} \neq \mu_{Block2} \neq \mu_{Block3} \neq 0$$

- The rainfall intensity in the runoff plots within the Tugen hills do not produce the same sediment yield during a rainfall event (do not have the same population means).

- The soils in the runoff plots (Blocks) are not homogenous i.e., the physical and chemical properties that includes bulk density, soil texture, percent Organic Matter (% OM) and percent Organic Carbon (% OC) play a significant role in sediment yield production in Tugen hills.

1.6 Justification of the study

Water Catchment areas are important and delicate examples of natural systems that must be approached with utmost caution when balancing exploitation and conservation, particularly in arid and semi-arid regions where soil erosion research is still required (Obando, 2004; Terer, 2005). When examining the economics of soil conservation, erosion control in both natural and agricultural contexts will be critical for preserving Kenya's levels of agricultural production (Karuku, 2018).

Identification of critical sites is required in order to prioritize erosion control funding, which are often limited. Soil erosion may pose a severe danger to food production and rural (as well as urban) livelihoods by 2030, especially in poor and heavily populated parts of the developing world. To meet their peoples' food demands in the long run, developing countries also advocate for policies that encourage soil conservation measures, land rehabilitation investments, and better land management approaches (Lussier *et al.,* 2020).

The study is in keeping with the Kenyan government's campaign to maintain the country's soil and water resources, as detailed in Vision 2030 declaration. Measures to be proposed at the study's conclusion are projected to improve the watershed soil fertility, resulting in increased agricultural output and sustainable riparian environmental protection among others (Alufah, 2012).

The Tugen Hills are one of the most productive locations in Baringo County. Because it impacts food supply, water resources, soil health, and grazing regions, soil erosion has a substantial impact on community livelihoods (Mbaabu, 2020).

1.7 Scope and Limitations of the Study

This research was conducted in Saimo catchment of Tugen Hills in Baringo County. Runoff plots measuring 4.8 m X 2 m were established and planted with Roscoco bean variety between the month of July and October, 2019. Sediment yield which is as a result of soil erosion by water was determined using MUSLE model. Only the MUSLE model input parameters were covered, other factors influencing soil erosion were none limiting.

CHAPTER TWO

LITERATURE REVIEW

2.1 Introduction

Hydrological studies of catchment areas give the information needed to assess the effects of diverse uses of the land and to plan and manage overall catchments. The consequences on soil and water resources of a bad land management method often leads to damaging impacts on water supplies, water supply and irrigation, and production of foodstuffs. (Boongaling *et al.,* 2018).

Changes in land utilization alter quality and quantity of streamflow, surface runoff, ground water recharge and soil loss, including sediment discharge relations, which can have an influence on channel processes and structure. Often these changes influence the structures of engineering, health and social welfare of downstream humans and animals.

Sediment yield is a significant measure of land degradation, severity and trends, as well as its historical, development, use and management features. Therefore, it is vital to study the environmental impacts of erosion and conservation practices, to create and evaluate erosion control strategies, to allocate conservation resources and to devise conservation regulations, policies and programs of soil erosion (Tsegaye and Bharti; 2021).

2.2 Tillage Practices

2.2.1 Conservation Tillage

The aim of the tillage preservation project is to provide a profit-making way in which wind and/or water erosion of the soil is minimized. The emphasis is on the conservation of the land, but it is also beneficial to preserve soil moisture, energy,

labor and even equipment. The method must ensure that conditions that resist erosion by wind, rain and flowing water are treated as tillage conservation. Either preserving the surface of the soil by crop residues and growing plants or keeping appropriate surface ruggedness and soil permeability, is a way of increasing water infiltration and hence reducing soil erosion (Niziolomski, J. C *et al.,* 2020).

Conservation tillage refers to any crop production technique that offers at least 30% residue cover after planting to decrease soil erosion caused by water, or 453.59 kilograms per acre of flat, small-grain residues. After planting, adequate erosion control sometimes necessitates more than 30% residue cover. Other conservation measures or structures may be needed as well. Conservation tillage systems include No-Till, Strip-Till, Ridge-Till, and Mulch-Till. (Tran, 2016).

i) No-Till

A no-till system is defined as a tillage system that leaves more than 70% of the surface covered by crop residue. The soil is left undisturbed from harvest to seeding and from seeding to harvest in this approach. The only "tillage" is the soil disturbance caused by a row cleaner, coulter, seed furrow opener, or other instrument attached to a planter or drill. Row cleaners are now available on many no-till planters to help eliminate residue from row areas. No-till planters and drills must be capable of cutting debris while also penetrating undisturbed soil (Niziolomski, J. C *et al.,* 2020).

ii) Strip-Till

It is a type of cultivation that takes place in between the rows. Strip-tilling is frequently combined with the application of anhydrous ammonia, dry fertilizer, or both in the fall. On some soils, particularly those with poor drainage, the no-till technique is supplemented with a strip-tillage operation in the fall to promote soil

drying and warming in the spring. As long as the required quantity of surface residue is left after planting, it is called no-till (Hayes, 2018).

Strip till has accelerated soil warming that results from removing residue as compared to no-till. Planting takes place as close as possible to the center of the berm than the soil between the rows. Maintenance of inter-row residue helps to provide the benefits of a no-till system, while the uncovered soil near the seed row reduces the negative effects of cold, wet soils often found in no-till systems (Niziolomski *et al.,* 2020).

iii) Ridge-Till

Ridge-till is also known as ridge-plant or till-plant. In this case, the soil is left undisturbed from harvest to planting except during fertilizer application. Crops are planted and grown on ridges formed in the previous growing season. Typically, ridges are built and reformed annually during row cultivation. A planter equipped with sweeps, disk row cleaners, colters, or horizontal disks is used in most ridge-till systems. Also crop residues are left between the ridges. Ideally, this leaves a residue-free strip of moist soil on top of the ridges into which the seed is planted (Licht *et al.,* 2005).

To reform the ridges, special heavy-duty row cultivators are needed. Before sowing, corn and grain sorghum stalks are occasionally shredded. Ridge tilling has become less popular in recent years, and it is now only used on limited plots of land. Driving through ridges during harvest is inconvenient, and the difficulties of creating and maintaining ridges, especially on slopes, as well as the requirement for specialized equipment and row cultivation during the season, all contribute to its decline (Niziolomski, *et al.,* 2020).

iv) Mulch-Till

Mulch-till includes any conservation tillage system other than no-till and ridge-till. In this method, soil is only disturbed before planting using tillage implements like cultivators and chisels. Residues are left on the surface without inversion. Herbicides and row cultivation control weeds. The tillage tools must be equipped, adjusted, and operated to ensure that adequate residue cover remains for erosion control, and the number of operations must also be limited. At least 30% of the soil surface must be covered with plant residue after planting (Kumar *et al.,* 2019).

2.2.2 Conventional Tillage

Conventional tillage is the sequence of operations used in a given geographic area to produce a given crop. With this system, mouldboard is used during cultivation. Later, secondary tillage follows with the use of disc or harrow. In the past, conventional tillage in Kenya included moldboard plowing, usually in the rainy season. The operations used vary considerably for different crops and in different regions. More recently, conventional tillage has changed to include the use of a chisel plow instead of a moldboard plow, and newer combination tools are replacing chisel plows. These implements leave more residue than traditional moldboard plows, but often not enough to qualify as conservation tillage (Mudamburi, 2017).

When traditional tillage was practiced in the past, the soil surface was essentially free of plant residue. This was especially useful when utilizing early planting equipment that couldn’t plant into residue. It also aided in the reduction of weed and plant disease problems by burying weed seed, disease-bearing crops, and weed debris prior to the implementation of current chemical treatment. Any tillage system that leaves the soil surface residue-free is referred to as clean tillage. Other procedures can also be employed to achieve a residue-free soil surface, particularly following a crop like

soybean, which leaves delicate, easy-to-cover residue. By eliminating all detritus from the soil's surface and modifying, soil erosion has been considerably accelerated. In lowlands, the likelihood of water erosion is reduced, but the risk of wind erosion is greater. Good tillage has been mostly replaced by improved planters, seed quality, and herbicides (Magdoff *et al.,* 2021).

2.3 Runoff Water Processes

It is important to understand runoff processes to make it easier to assess surface and groundwater risks in terms of quality and quantity. It aids in the quantification of water resources for water allocation, hydropower production, hydraulic structure design, environmental flows, drought and flood control, and water quality applications (Saatsaz. 2020). With proper understanding of these processes leads to the development of tools such as hydrograph separation techniques that identify runoff components in stream water, flow paths, residence times, and contributions to total runoff (Yang *et al.,* 2020).

In tropical, dry and semiarid environments, it is still necessary to discover runoff production methods, as much less has been explored. Sporadic, high-energy and low frequency precipitation characterize arid and semi-arid environments. Drought spells may endure for years and precipitation events range between a few mm and hundreds of mm each annum. High storms can produce most, if not all of the season (Scholes, 2020). These events can also increase erosion, reduce soil infiltration capacity and enhance surface runoff (Camarasa- Belmonte and Soriano, 2014).

Lack of precipitation may result in reduced to non-existent groundwater recharge. Compared to humid regions, where evaporation is generally limited by the amount of

energy available, evaporation in arid and semi-arid areas is usually limited by water availability in the catchment (Narantsogt and Mohrlok, 2019).

2.4 Soil Loss Tolerance

Tolerance to soil loss (allowable loss of soil or sustainability) value, T, serves to determine if a river is potentially exposed to erosion and sediments productivity loss and is often a final criterion for erosion control and an indicator of soil quality. It is also a condition for soil productivity and environmental conservation (Young *et al.*, 2005).

Soil loss tolerance has received increased attention since it is directly related to the fundamental soil erosion problems. Some of the fundamental and applications of great importance for the development of land erosion control measures in agricultural and other lands. Therefore, it must be determined scientifically and rationally for the assessment of no excessive erosion regions and erosions and for the determination of a T value. However, a high T-value reduces soil conservation costs and may result in over erosion of earth, resulting in a number of difficulties, such as soil fertility and productivity decline, soil degradation, eco-environmental deterioration, and so on.

Cook (1982) explored the questions of T value proposed by the US department of Agriculture's Soil Conservation Service, and Schertz (1983) made a complete assessment of the early studies of T value and concluded that ''soil loss tolerances are not sacred." They should, however, be amended only when adequate research suggests it or when social circumstances demand it. Johnson (1987) later provided a review of T value. However, no additional reviews were discovered. As a result, discussing soil loss tolerance is critical and necessary (Duan *et al.,* 2017). According to Lufafa *et al*., (2003), the average tolerable soil loss threshold is 10t/ha/y.

2.5 Soil Sampling Methods

When trying to get a representative soil sample, land variability is a huge problem. This difficulty can be addressed through the approach utilized to test an area. During a site evaluation, information obtained may help to choose the best strategy for a given area. A random composite sampling, guided random composite sampling, benchmark sampling, land-based benchmark sampling, and grid sampling are some of the sampling techniques that can be used (Lin *et al*., 2013).

The process of obtaining samples in a random pattern over a field while avoiding anomalous or problem soil locations is known as random composite sampling. This method is best suited for fields with fewer than 30 ha that have recently been consistently cropped and have little natural variation. It is the most prevalent sampling method currently in use in Kenya. Collect cores from 15 to 20 sites for random sampling and split each core by depth to obtain representative bulk samples for each depth. A modified variation of a random sampling approach is directed or managed random sampling. It is appropriate for fields where identifying a single dominant area is challenging. Depending on the number of management zones, a single field may necessitate many bulk samples. This method may also be appropriate for hummocky terrain and strip-crop management (Zhang and Hartemink, 2017).

Benchmark sampling is choosing a modest (30 m x 30 m) representative site on a field. Within the benchmark region, select probe sampling locations in a grid pattern and generate a composite sample for each soil depth. Sampling from the same small area each year lowers sampling variability and allows for more accurate reflection of changes in soil nutrient levels from year to year. A Global Positioning System (GPS) tracker or any other suitable site may be used to represent the field. If a single site

does not adequately represent a field, it may be necessary to maintain multiple benchmark areas (Lin *et al*., 2013).

Direct benchmark technique entails defining a number of benchmark regions and management zones depending on geography or other factors. When key sections within fields have distinct and well-defined moisture characteristics, this technique might be applied.

Grid sampling is the most intensive and costly sampling approach. It employs a methodical approach to uncover fertility trends and assumes that there is no topographic basis for fertility patterns to vary within a field. A field is divided into small blocks for sampling. The main advantage of this method is that a field map for each nutrient can be created, allowing for variable-rate fertilizer application. The cost of evaluating the requisite number of samples is uneconomical for many producers (Zhong *et al.*, 2017).

2.6 Agricultural Production in Kenya

The importance of agriculture to the economy cannot be emphasized. In 2017, the industry was responsible for 31.5 percent of the country's GDP, 75 percent of the labor force, and more than half of all export revenue. Agriculture sector growth, on the other hand, has decreased over the last five years, falling from 5.4 percent in 2013 to 1.6 percent in 2017. Indeed, the country's food output has declined during the last five years. Drought, limited agricultural land expansion, low and declining soil fertility, insufficient use of quality seeds, delayed supply, high fertilizer prices, and pests may all contribute to a reduction in food production (Jane, 2009).

According to the 2017 Global Food Security Index, Kenya is food insecure, ranking 86th out of 113 countries, with food cost, availability, quality, and safety being an

issue. Kenya imports the majority of its cheap key food commodities, including wheat, maize, rice, beans, potatoes, sugar, and milk, according to the country's food balance. It should be noted that agriculture is a devolved activity, which may explain the drop in resource allocation that could have been used to help farmers boost agricultural yields at competitive pricing. Soil erosion is bound to increase in future as minimal or no resources are deployed to help put up interventions that conserve soil and water which are critical resources for agricultural production. This mandates that any interventions aiming at increasing agricultural performance be implemented in collaboration with county administrations (Jane, 2009).

The ideal temperatures for growing common beans in Kenya range from 17.5 to 27^{o} C. Flower buds are more likely to fall at temperatures above 30^{o} C, while seeds are rarely developed at temperatures above 35^{o} C. They are vulnerable to night frost. Common beans varieties are often planted at elevations ranging from 600 to 2000 metres above sea level (ASL). Moderate, evenly distributed rainfall (300-400 mm per crop cycle) is required, although dry weather during harvest is crucial (Nasidai, 2015).

Some of the most common bean varieties are Canadian wonder for medium rainfall locations, Mwitemania for low to high rainfall areas, Red haricot for high rainfall areas, Rose coco for medium-high altitude places, Wairimu dwarf for low rainfall areas, and Mwezi moja for low-medium rainfall areas. Prepare the land to a fine tilth 2-4 weeks before the commencement of rains to allow organic materials to fully decay. Plowing can be accomplished with hoes, oxen plows and tractors. Planting must be done as soon as the rains begin, after minimum of 30mm of rain has fallen. The seed rate is 2 seeds per hole that is, about 40-50 kg/ha (16-20 kg/acre). Plant at 45 cm between rows and 20 cm between plants for a single crop. Beans are ideal for intercropping and can assist in nitrogen fixation to other crops (Wairegi *et al*., 2015).

Use of farmyard manure (6-8 ton/acre) is recommended especially where soils are low in organic matter. When inter-cropping with maize, interplant two bean rows at 15 cm intervals between the maize rows and put one seed per hole. The fertilizer should be thoroughly mixed with soil before planting to avoid scorching effect.

2.7 Soil Erosion by Water

Soil erosion by water comprises both rain and water rushing across the soil surface. The primary detaching agent is rain splash, but the main carrying agent is water flowing. This activity appears to have been observed by humans from the early Chinese civilizations. Soil erosion is a major global soil degradation issue that affects humans. According to FAO (2010), soil erosion affects between 25 and 30 percent of Africa's total cultivable area. Soil loss due to water erosion is always accompanied by nutrient losses in the soil (Vaezi, 2017).

In the case of water-induced soil erosion, both rain splash and water moving across the soil surface separate and transfer the detached particles, but rain splash is the most important detaching agent, whereas running water is the primary carrying agent. The movement of soil particles induced by running water is referred to as interrill and rill erosion, whereas rain splash erosion is caused by the direct impact of falling droplets.

Water flowing as a shallow sheet ("overland flow") and removing soil by "digging out" channels of increasing depth and/or width is referred to as interrill erosion, whereas rill erosion refers to water flowing as a concentrated flow and removing soil by "digging out" channels of increasing depth and/or width is referred to as rill erosion. A cross-sectional area of at least $1ft^2$ is widely acknowledged as a criterion for separating gullies from rills, and gullies account for around 80% of detachment/soil loss on larger scales (Stolte, 2015).

Water flowing downslope through the soil matrix ("interflow"), as well as water flowing over the soil surface as previously indicated, can detach and move soil particles, especially through macropores or underground pipes. These subsurface erosion mechanisms are especially common in peatlands and places with fabricated subsurface drainage systems (Morgan, 2009).

Because the land is humanity's primary source of subsistence, soil erosion is a major global soil degradation problem that affects humans. Land use changes, on the other hand, have been identified as having the potential to increase soil erosion everywhere over the world (Vanwalleghem *et al*., 2017). Degraded soil is unproductive, and the degree of damage to the land determines how productive it is. Soil degradation is happening at an alarming rate all across the world. According to the FAO, soil erosion affects between 25 and 30 percent of Africa's total cultivated land (2010). Soil erosion has affected over 70% of Kenya's land surface, with varying degrees and types of erosion affecting different parts of the country. According to FAO (2010), if no conservation measures are implemented, the total area of rain-fed agriculture in developing countries in Africa, Asia, and Latin America will drop by 544 million hectares over time owing to climate.

Soil loss due to water erosion always precedes the loss of essential soil nutrients. This is because erosion is selective, with fine soil particles, which are significantly richer in soil nutrients, being more susceptible to erosion. Only a few of the human activities that contribute to increased erosion are urbanization, agricultural operations, construction, grazing, and logging. The cost of water-induced soil erosion is substantial since it damages natural resources. Detachment, migration, and deposition of eroded particles are all examples of water erosion. Raindrop impact and flowing water shear stress are eroding factors that cause soil to separate. Surface flow, as well

as concentrated flow in rills, gullies, and streams, carry runoff and unattached particles down the hill (Tian *et al*., 2022).

2.7.1 Soil erosion mechanism

Various soil detachment occurs in rills and interill regions, where rills are defined as small erodible channels that can be erased by conventional plowing. Raindrop impact is the primary source of detachment in interill regions, and the degree of detachment is proportional to soil structure and texture, rainfall intensity, and land cover. Runoff also causes soil particle separation when the applied load exceeds the critical shear stress of the soil. Interill erosion is relatively independent of slope length because raindrop impact has a significant influence (Hould-Gosselin *et al.*, 2015).

Soil detachment is described as the dislodgement of soil particles from the soil mass at a specific point on the soil surface caused by the erosive forces of rainfall and runoff, which can result in the formation of rills and gullies. Because the mechanism of soil dissociation caused by interill and rill erosion differ, they are treated as discrete sub-processes in process-based erosion models. Detachment in interill erosion is caused and exacerbated by raindrop effects, with raindrop impacted overland flow serving as the primary transportation medium (Tian *et al.*, 2022).

Rill erosion, on the other hand, is thought to be the most important mechanism of sediment formation on steep slopes. It is mostly generated by overland flow, whereas the impact of raindrops on detachment is negligible. The effect of runoff water on soil detachment capability has been widely examined under various environmental conditions, both laboratory and field tests employing hydraulic factors such as flow regime, discharge, slope gradient, flow depth, velocity, friction, and sediment content.

The resistivity of the topsoil or the erodibility of the soil also influences the erosion process by overland flow (Wang *et al*., 2019).

Topsoil resistance is mostly determined by soil parameters and vegetation features. Soil type, texture, and soil physiochemical properties such as porosity, bulk density, cohesion, clay content, aggregate stability, organic matter content, soil moisture, and infiltration rate have been shown to have strong relationships with soil detachment capacity. It has also been discovered that as soil organic matter, moisture content, and bulk density increase, soil detachment also increase. Any change in soil characteristics caused by farming, land use change, soil consolidation, or vegetation expansion would undoubtedly affect soil detachment by overland flow (Wang *et al.*, 2019).

Vegetation plays an important role in the soil detachment process by modifying soil parameters during the growth period, hence indirectly influencing infiltration rate and soil erosion. Root networks have a significant role in preventing soil erosion and increasing soil stability by connecting soil particles at or near the soil surface, reducing soil detachment. It has been found that the power of vegetation roots to minimize soil erosion is more than previously thought. Various root metrics have been measured and employed in different experiments to mimic the impacts of roots on soil detachment capacity by overflow. Root structure has an impact on the erosion-reducing properties of roots. Taproots, on average, have a lower erosion rate than fibrous roots (Usharani *et al.,* 2019).

Organic soil crusts, which are thin coatings of biological and mineral particles at the soil surface, influence soil detachment by affecting soil strength, water infiltration, and runoff. Furthermore, soil surface resistance to water varies with landscape

position, influencing runoff, drainage, soil erosion, and soil formation, and so influencing the soil detachment process overland flow (Shanshan *et al*., 2018).

2.7.2 Accelerated Soil Erosion

Water, wind, and gravity are the primary erosive factors. Erosion is a process that is frequently exacerbated by human land-use activities. Accelerated erosion is defined as soil loss that occurs in addition to natural erosion. It is typically connected with changes in natural vegetation or soil conditions and is primarily induced by wind and water (Assaye, 2020).

The initiation phase of the erosion process is splash erosion. It happens when droplets strike bare earth. Individual soil particles are splashed onto the soil surface as a result of the explosive impact thus breaking up soil aggregates. The splattered particles can travel up to 1.5 m from the point of impact and climb up to 60 cm above the ground. Because the particles obstruct the crevices between soil aggregates, the soil creates a crust, reducing infiltration and increasing runoff. The loss of soil in thin layers caused by raindrop impact and shallow surface flow is known as sheet erosion. It causes the loss of the finest soil particles, which contain the majority of the soil's accessible nutrients and organic matter. Soil loss is so gradual that it frequently goes unnoticed, but the cumulative impact accounts for enormous soil losses (Douglas, 2020).

2.8 Sediment Transport and Deposition

When transport capacity of flowing water falls below the entrained sediment load being transported, deposition occurs. Flow velocity controls the transport capacity of flowing water, which is reduced by any factor that reduces velocity, such as negative filter strips, terrace, channels, and check dams. Toes of concave slopes and filter strips are common locations for sediment deposition. Along the length of the slope, the

three components of erosion namely: Detachment, transportation and deposition interact. Flow at transfer capacity does not detach any additional soil unless the velocity increases. Furthermore, the amount of soil carried downslope is proportional to the smaller of transport capacity and accessible soil for transport (soil detached locally plus received from upslope) (Husic *et al*., 2020).

2.8.1 Sediment Delivery Ratio

Sediment delivery ratio (SDR) is defined as the supply from a region divided by the area's total erosion. It is given as a percentage and shows the watershed's efficiency in transferring soil particles from erosion zones to the point where sediment yield is assessed. Some of the eroded soil may be deposited while travelling to downstream place of interest. As a result, the USLE model cannot be used to properly predict the quantity of sediment reaching river basins (Dinka, 2020). To account for these processes, the SDR can be used to estimate the total sediment brought out of the surface of Tugen Hills. The SDR values for a given area are influenced by factors such as watershed physiography, sediment sources, transportation systems, the texture of eroded material, land cover, and so on. From literature, the average channel slope is more significant than other parameters in estimating SDR, which is expressed as follows:

$$SDR = 0.627SLP^{0.403} \tag{2.1}$$

Where the SLP (%) is the slope of the mainstream channel.

In circumstances where data is scarce, this equation could be used to provide an acceptable estimate of the SDR (Onyando *et al*., 2005).

2.9 Erosion Prediction

Soil erosion models are primarily used to calculate soil loss. Different models have different operational requirements and concepts. There are several techniques to modeling soil erosion. These approaches differ in terms of scale, both in time and space, amount of data required, processes modeled, mathematical representation of processes, and finally, output type. The most basic erosion models, such as the Universal Soil Loss Equation (USLE), estimate gross erosion from a given area but do not indicate how much erosion leaves that area. Sediment deposition is not explicitly modeled in such models.

More advanced models, such as physically based models, include mathematical correlations based on degraded material's physical properties. These models characterize the processes of detachment, transport, and deposition and generate spatially variable estimates of detachment, deposition and sediment production.

The Agricultural Catchment Research Unit - Nitrates, Phosphorous and Sediments (ACRU-NPS) Model is a semi-distributed model, in which lumped sub-catchments are spatially distributed based on spatial variability of land-use, topography, precipitation and soil characteristics. The ACRU-NPS model simulates runoff, sediment and nutrient (NO3 and P) production in agricultural catchments, and can be used to evaluate the impact of farming practices and land-use changes on crop yields, water discharge, sediment and nutrient loads (Kollongei and Lorentz, 2015). Agricultural Non-Point Source Pollution Model (AGNPS), an event-based distributed model in which physical or chemical constituents are routed from their origin within a cell to the stream network or the watershed outflow, is an example of a distributed watershed model. CASC2D is another distributed model that employs an infiltration excess formulation. CASC2D employs finite difference techniques to solve the

equation of mass, energy, and momentum flow between cells. This model is continuous and is appropriate for small-scale applications.

Systeme Hydrologique European (SHE) is a process-based spatially distributed (PBSD) system for modeling coupled surface and subsurface water flow and sediment transport in river basins. The model requires extensive input data and parameters (Yuan *et al.*, 2020).

Two other distributed models stemmed from SHE, Système Hydrologique Européen TRANsport (SHETRAN); and European Hydrological System Model (MIKE-SHE) with the main difference between the two models being the way subsurface flow is modeled. SHETRAN can model 3D flow in variably saturated soils, whereas MIKE-SHE simulates only vertical flow in partially saturated soils (Refsgaard *et al.*, 2010).

The increasing availability of spatial data in the form of Geographic Information System (GIS) and remote sensing coverages is one element contributing to the resurgence of distributed hydrologic and erosion modeling. Geographic information systems are increasingly being employed in distributed watershed modeling, with varying degrees of involvement. GIS modules are mostly used to study geographic properties of watersheds for use in hydrologic models (Srivastava and Chinnasamy, 2021).

2.10 MUSLE Model

The Modified Universal Soil Loss Equation (MUSLE) is a model that is experimentally driven and is based on the Universal Soil Loss Equation (USLE). It simulates erosion and sediment output using storm-based runoff volumes and peak flows. It varies from USLE in that it is entirely dependent on rainfall as a source of erosive power. MUSLE was utilized in this study to estimate storm-wise sediment

yield for plots created within freely grazed land and manually harvested areas in Baringo. Because most watersheds, particularly minor ones, are frequently un-gauged, determining sediment yield is impossible owing to lack of data. MUSLE is the only soil erosion forecasting model that account for a lack of rain gauge data (Arekhi, 2011).

The USLE model was developed as a tool for agricultural land maintenance and has been widely utilized globally. The fundamental shortcoming of the model and its improved version, RUSLE, is that runoff is not directly considered, despite the fact that erosion is dependent on sediment discharged with the flow, which varies with runoff and sediment quantity (Djoukbala *et al*., 2019).

MUSLE can predict sediment yields for specific storm events by using runoff factors rather than rainfall erosivity as the main driver. This provides a better knowledge of the water-induced erosion process. This approach also predicts sediment yield more accurately and eliminates the requirement for delivery ratios. Furthermore, MUSLE is simple to use and requires only a few variables (Benavidez *et al.*, 2018).

MUSLE optimizes the parameters of a hydrologic model to estimate sediment yield (Figure 2.1). Williams and Berndt (1977) analyzed 778 distinct storm occurrences in 18 catchments with areas ranging from 15 to 1500 hectares in an attempt to establish hydrological processes of sediment yield. The derived resulting equation that best fits the data was given by:

$$S_y = 11.8(Q.q_p)^{0.56}K.LS.C.P \qquad (2.2)$$

where:

S_y = sediment yield (tonnes)

Q = volume of runoff (m^3)

q_p = peak flow rate (m^3/s)

K = soil erodibility factor (t.ha.hour/ha.MJ.mm);

LS = slope length and steepness factor;

C = cover management factor;

P = support practice factor.

According to Simons and Sentürk (1992) the MUSLE coefficients, α_{sy} and β_{sy}, are location specific and must be determined for specific catchments in specific climatic zones. Though very little research has been undertaken on calibrating these runoff energy factors (Kienzle and Lorentz, 1993) the originally calibrated values, α_{sy} = 8.934 and β_{sy} = 0.56, for catchments in Texas, Oklahoma, Iowa and Nebraska in the USA by Williams (1975) are commonly used when Q_v and q_p are in SI units. Lorentz and Schulze (1995) used values of $\alpha_{sy} = 11.8$ and $\beta_{sy} = 0.56$ which have been used extensively with varying degrees of success in South Africa and similar approach was utilized in Saimo catchment in Baringo. The storm volume, Q_v (m^3), for the event is related to the detachment process while peak discharge, q_p (m^3/s), is associated with sediment transport (Kollongei and Lorentz, 2015).

The MUSLE approach is primarily used in ACRU-NPS to estimate sediment yield from individual rainfall events at a catchment scale because it has been developed as a hydrologically driven simulator (Lorentz and Schulze, 1995). The MUSLE method is thus well suited for use with modified SCS technique to generate storm flow in an event based ACRU-NPS model. MUSLE equation allows prediction of sediment yields directly without using sediment delivery ratio.

The factor K, LS, C and P are determined from empirical equations and experimental observations in ACRU-NPS, various options are offered to estimate these parameters depending on the level of data and information available. These options have been developed from the USLE and the RUSLE manuals, and for modelling in South Africa from local experimental observations (Lorentz and Schulze, 1995).

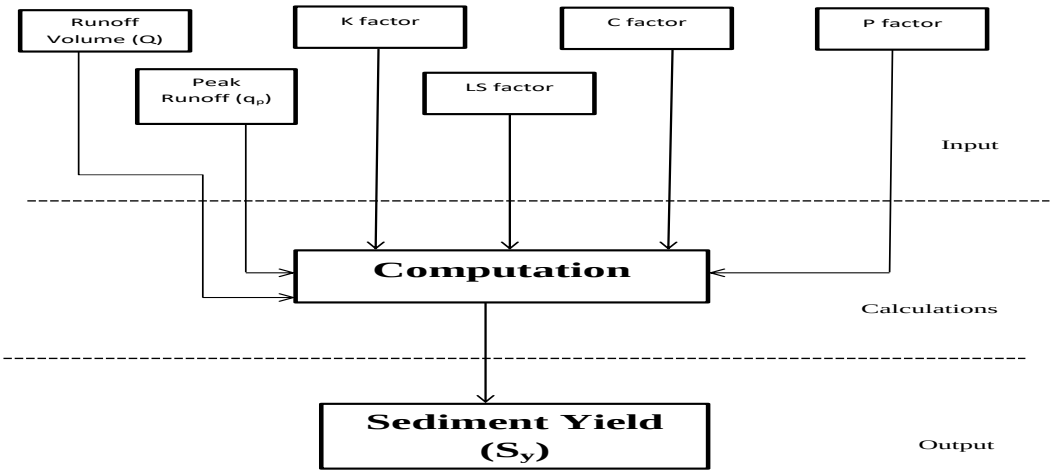

Figure 2.1: Program Flow chart for MUSLE Module (Source: Author)

2.10.1 K-Factor

The K-factor depicts how simple the soil is removed by splash during surface water and rainfall. It also shows the change in soil per unit of external force. This component accounts for the effects of soil qualities on soil loss during storm occurrences on sloping terrain and is connected to the integrated effect of runoff, rainfall, and infiltration. To measure soil erodibility in tropical soils, poor soil aggregates, modified silt, sand, and the appropriate base concentration are used. The K-factor determined from the USLE nomograph is appropriate to tropical soils with kaolinite as the primary clay mineral, but it is less useful when Vertisols predominate (Mati *et al*., 2001). Soils in Saimo catchment is predominantly leptosols.

2.10.2 Topographic Factor (LS)

The “topographic factor, LS”, refers to the impact of slope length and gradient on the severity of the erosion process. The LS-factor takes into account the erosion effects of slope length and gradient. For calculating LS on uniform slopes, USLE offers conversion tables. Soil loss is faster on steeper slopes than on longer slopes. Field measurements are the most accurate ways to determine them. For the examined watershed, however, fieldwork is both time-consuming and labor-intensive (Southgate and Disinger, 2019).

2.10.3 Cover management factor (C)

The crop factor, C, is a metric that assesses the impact of all interconnected cover and management parameters. It can range from zero for well-protected soils to 1.5 for finely tilled and textured surfaces that are prone to rill erosion. USLE has a large crop database, including several tropical crops, that can be used to calculate the C-factor, especially when plant growth parameters are known, or the user can create their own file from experimental results (Thomas *et al*., 2018).

Assessment of soil erosion and sediment yield in Tugen Hills, Baringo County, Kenya, using GIS, and Remote Sensing, RS, cropping and management and the effect of ground, tree, and grass coverings on minimizing soil loss in non-agricultural circumstances are represented by the C-factor in the USLE. It calculates the total impact of all interconnected cover and crop management factors. Allocating published C values to matching land cover classes can be used to calculate the C-factor. Remote sensing allows for the assessment of land cover at any location on the planet’s surface. Tugen Hills has been observed and categorized as forest, agriculture, grass, shrub, bare soil, urban and traffic, and underused, among other things. The C map will

be created by giving representative values to classified land cover classes from USLE reference tables (Kebut, 2019).

2.10.4 Practice factor (P)

The practice factor (P), is the ratio of soil loss caused by a certain support method to the loss caused by up and downslope tillage. By changing the flow pattern, gradient or direction of surface runoff, as well as lowering the amount and rate of runoff, these measures have a corresponding impact on erosion. The P-factor ranges from roughly 0.2 for reverse-slope bench terraces to 1.0 when no erosion control measures are in place. Contouring (tillage and planting on or near the contour), strip cropping, terracing, and subsurface drainage are examples of support practices used on croplands (Gwapedza *et al*., 2021).

2.11 Conceptual Framework

There are a number of variables that are determining factors of sediment yield. The independent variables are runoff volume, peak runoff, soil erodibility, slope length and steepness, cover management and support practice while the dependent variable is sediment yield. Figure 2.2 presents conceptual framework for MUSLE model.

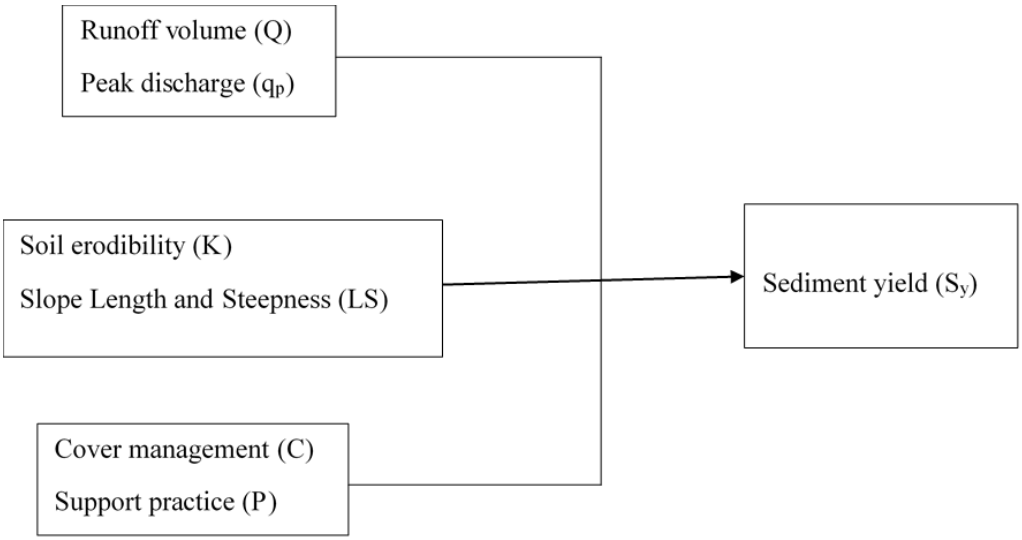

Figure 2.2: Conceptual Framework

CHAPTER THREE

MATERIALS AND METHODS

3.1 Study area

Runoff plots were set up in Tugen hills within Saimo catchment at the location (0.5842^0 N and $35.74\ 00^0$ E, with an altitude of 1625 m above sea level) in Baringo County (Fig 3.1). Rainfall is of bimodal type with long rains occurring between April to August and short rains between September and November with an average of 1000 mm/yr. Maximum average temperatures in the area is 28^0 C occurring between February and March while minimum average temperatures is about 11^0 C and occurs between the months of December and January. Soils here are majorly classified as Leptosols (weak developed shallow soils). The area is relatively steep with dominant agricultural practices being growing of maize, fodder and small-scale livestock farming (Kimani *et al*., 2014). The research site is approximately at a distance of 15 km from Kabarnet town.

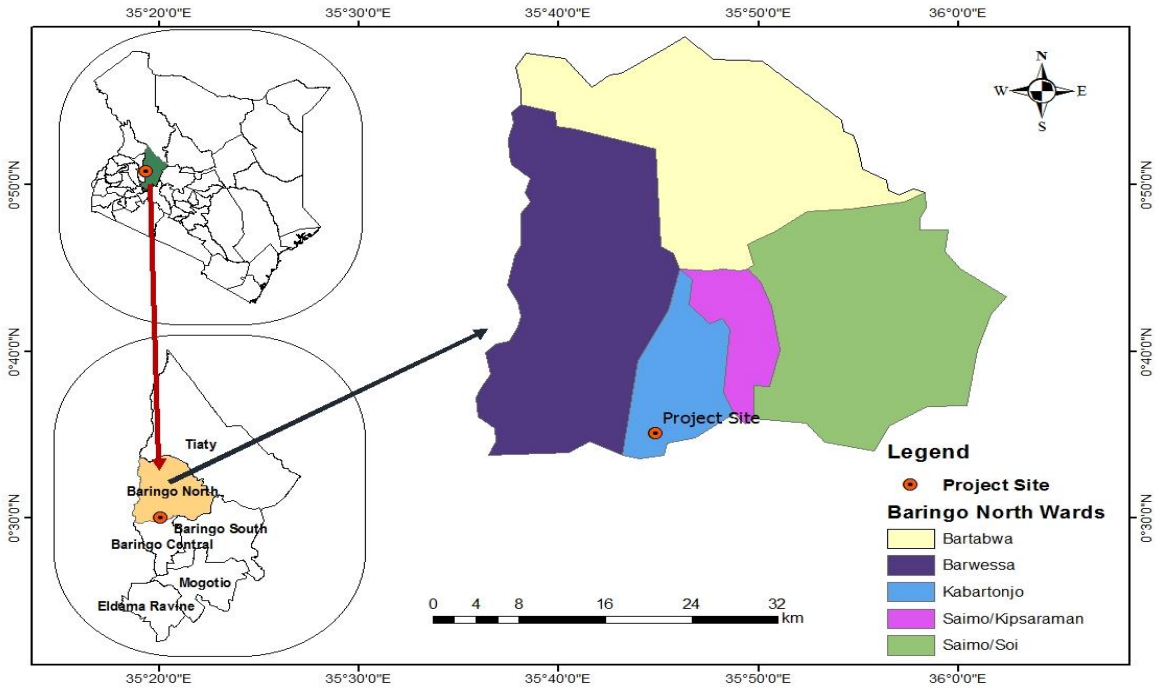

Figure 3.1: Location Map of the Project Site

Tugen Hills are a group of hills in Baringo County. They are found in Kenya's central-western region. The Tugen Hills are one of the few sites in Africa that have a sequence of deposits dating from 1 to 4 million years ago, making them a valuable location for studying human (and animal) evolution. Richard Leakey and others have found a 1.5-million-year-old elephant skeleton (1967), new species of monkey (1969), and fossil remains of 1 to 2 million-year-old hominids (Senut *et al*., 2001). Saimo catchment forms part of Tugen hills located in Baringo North Sub-County.

3.2 Treatments and Experimental Design

The treatments were comprised of three tillage practices (conventional, mulching and control) in a randomized complete block design (RCBD), with three replicates. Each replicate had 3 treatments and a unit plot measured 4.8m×2m. The distance between plots was 30 cm (Fig 3.2). The treatments were allocated by casting lots. Assignment started from West to East. The runoff plots were sloping from North to South. In Figure 3.2, B stands for Blocks. The area was divided into three blocks. T in the figure stands for treatments, T1 (no mulch), T2 (mulched) and T3 (Control, left). Spacing between the blocks was made as 0.4 m.

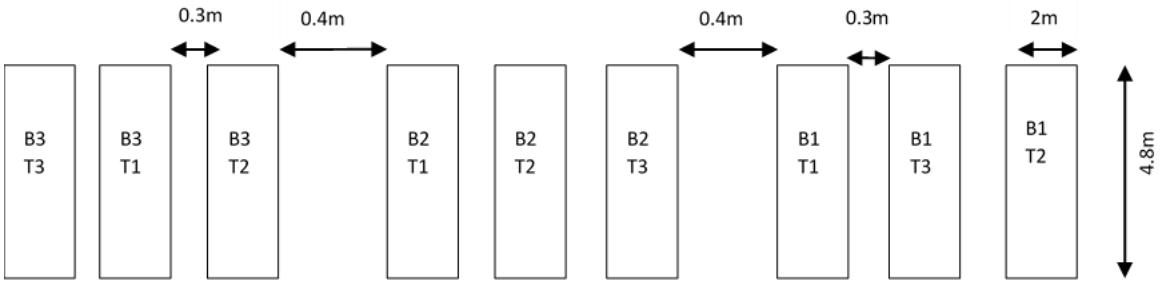

Figure 3.2: Experimental Layout

3.3 RCBD Two-Away ANOVA Model:

Considering experiments involving only two factors i.e. ‘a’ levels of factor A and ‘b’ levels of factor B.

FACTOR B

FACTOR A	1	2	……	b
1	y_{111} y_{112} y_{113} y_{11n}	y_{121} y_{122} y_{123} y_{12n}	……	y_{1b1} y_{1b2}
2	y_{211} y_{212} y_{213} y_{21n}	y_{221} y_{222} y_{233} y_{22n}		y_{1b3} y_{1bn} y_{2b3} y_{2bn}
……	……			
a	y_{a11} y_{a12} y_{a13} y_{a1n}			y_{ab1} y_{ab2} y_{ab3} y_{2bn}

$$y_{ij} = \mu + \tau_i + \beta_j + (T\beta)_{ij} + \varepsilon_{ijk} \qquad (3.1)$$

i = 1, 2, ……..a (Factor A)

j = 1, 2,……b (Factor B)

k = 1, 2, …….. n (Replication)

where:

y_{ijk} – observation taken under the i^{th} level of factor A and j^{th} level of factor B in the kth replicate

μ – overall mean

τ_i - effect of the i^{th} level of factor A

β_j – effect of the j^{th} level of factor B

$(\tau\beta)_{ij}$ – effect of the interaction between τi and βj

ε_{ijk} – Random error component (CT)

ε_{ijk} ind ~ N (0, σ2)

$$C_T = (\sum_i^a \sum_j^b \sum_k^c y_{ijk})^2 = \frac{y_{...}^2}{abn} \quad (3.2)$$

$$SS_{Total} = \sum_i^a \sum_j^b \sum_k^n y_{ijk}^2 - CT \quad (3.3)$$

$$SS_A = \sum_{i=1}^a \frac{y_{i..}^2}{bn} - CT \quad (3.4)$$

$$SS_B = \sum_{j=1}^b \frac{y_{.j.}^2}{an} - CT \quad (3.5)$$

$$SS_{AB} = \sum_i^a \sum_j^b \frac{y_{ij.}^2}{n} - CT - SS_A - SS_B \quad (3.6)$$

$$SS_E = SS_{Total} - SS_A - SS_B - SS_{AB} \quad (3.7)$$

Differences in the means of observed sediment yields from the control plots were analyzed using two-way ANOVA. This provided a range of values for the difference between the means of sediment yields from the runoff plots. Recommendations were made based on the results.

3.4 Slope

The general gradient of the project site was determined by use of line level. Levels of three points within the proposed project set up area were taken and an average obtained. Verification was done by using a clinometer.

3.5 Installation of Runoff Plots

In preparation for installation of runoff plots, a leveling exercise was carried out to establish the general slope of the area. Galvanized metallic sheets of gauge 24 were used to construct all the runoff plots. These sheets were cut into strips of 30cm in thickness and buried 10cm below the ground surface. The border joints were then flapped firmly together and soil compacted gently along the boundary walls. An apron of 20cm was installed downstream of the runoff plot to cover the entire width

providing smooth connection between the ground and the runoff collector. The collector was then overlapped with the apron to concentrate and direct the runoff and sediments through a delivery pipe of 4 inches to a covered collection tank of 20 litres capacity (Figure. 3.3 (a) and (b)).

Runoff plots of 4.8m long by 2m wide were developed. The plots were established adjacent to one another with the long axis (length) perpendicular to the contours. The plots were isolated using metallic plain sheet partitions. The runoff was channeled out of the plot by means of a metallic apron and a 4'' PVC pipe to a collection tank at the downslope end. A cut off drain of 0.25% slope was done upstream to safely discharge runoff from entering experimental site. In the downstream, a retention ditch of 0.8m wide and 0.6m deep was done to allow the positioning of the collection container.

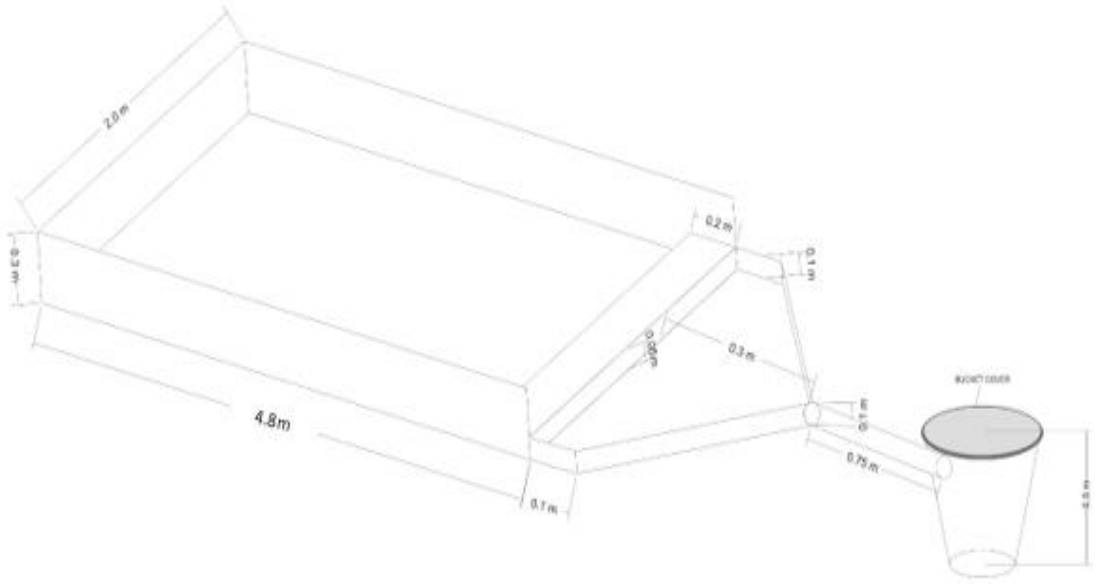

(a)

(b)

Figure 3.3: (a) Complete Runoff plot (b) Prepared Run-off plots

3.6 Soil Sampling

Soil samples were collected randomly in three points within the experimental site. Soil sample rings were used to collect undisturbed soils at 0-10 cm and 20-40 cm. The soils were then analyzed for physical properties which include texture, structure, bulk density and hydraulic conductivity and chemical properties carbon and organic matter.

3.7 Land preparation

The plots were ploughed conventionally using hand hoe (“Jembe”) along the contour after the installation of boundary metal sheets. An average plough depth of 20cm was achieved. Extra care was taken not to move the soil further from its original position and not to disorientate the boundary sheets.

3.8 Bean crop

3.8.1 Bean Varieties

Common bean (*Phaseolus vulgaries*) varieties grown in Kenya include Rose coco, mwitemania, mwezi moja and wairimu. Rose coco variety type was planted on the

two plots and one unploughed plot left as control. These plots under bean crop as plant cover and control (no crop planted) was replicated three times.

3.8.2 Planting and Spacing

Two seeds were placed in a 2.5cm-deep hole. DAP fertilizer was applied at a rate of 50kg/ha. A spacing of 45cm between the rows and 20cm between crops was maintained in all the plots planted.

3.8.3 Management Practices

Weeding was done by use of hand hoe two weeks after germination and on the start of flowering stage on the plots with no mulch. Pesticide to control black bean aphids was sprayed in all plots with mulch and no mulch.

3.8.4 Mulching

Hay grass was used as mulch material. The mulch was placed uniformly in the entire plot with mulch treatment one and half weeks after germination and at about 3.5 inches above the ground.

3.9 Runoff and Sediment Sampling

3.9.1 Sediment collection

Runoff were collected and recorded after every rainfall event. The automatic rain recorder was used and manual rainguage (Figure 3.4b) used as a check. After every rainfall event, runoff generated was collected in 20 litres containers, emptied and the measurements recorded. Prior to collection of the runoff and measuring, the apron part of the runoff plot was cleaned thoroughly using the runoff water already in the container. After which, the mixture was thoroughly mixed and measured to record total volume of runoff. The portion of this runoff was taken to the laboratory for measurement of sediments.

Figure 3.4: (a) Run-off water collection and (b) Rain gauge

3.9.2 Sediment analysis

In the laboratory, a representative 200ml of runoff sample was thoroughly shaken, and 5ml of Hydrochloric acid added to promote the flocculation of the suspended materials. The mixture was then left overnight to allow the suspended solids to settle completely, and the supernatant water was carefully discarded. The remaining wet sediments was oven dried overnight at 105°C, and sediment concentration was calculated by dividing the dry mass of the sediments by the sample volume.

3.10 Determination of MUSLE input parameters

The MUSLE model is given by equation 2.2 as described below.

$$S_y = 11.8(Q.q_p)^{0.56}K.LS.C.P$$

where:

S_y = sediment yield (tonnes)

Q = volume of runoff (m^3)

q_p = peak flow rate (m^3/s)

K = soil erodibility factor (t.ha.hour/ha.MJ.mm);

LS = slope length and steepness factor;

C = cover management factor;

P = support practice factor.

3.10.1 Volume of runoff (Q)

Runoff volume from the plot (micro-catchment) per rainfall event was obtained by measuring the contents of the collection tank after the rain and overland flow stopped in every plot.

3.10.2 Peak flow rate (q_p)

To estimate peak flow rate, equation (*3.8*) was used:

$$q_p = \frac{1}{3.6} CiA \tag{3.8}$$

Where;

q_p = Peak runoff rate (m^3/s)

C = Runoff coefficient

i = Rainfall intensity (mm/h)

A = Area (km^2)

Rainfall data was obtained from automatic rain recorder installed within the experimental site. A manual rain gauge was installed next to the automatic rain gauge to supplement. An automatic rain gauge allows for rainfall intensity to be directly read while the manual rain gauge can be used to supplement the rainfall data in case of failure of the automatic rain gauge or for checking purposes. Runoff coefficient (C)

was obtained from tables in appendix III while the area, A was determined by dimensions of runoff plot.

3.10.3 Soil Erodibility, K-factor

The percent-modified silt (0.002–0.1 mm), percent-modified sand (0.1–2 mm), base saturation, percent unstable aggregates, and percent very fine sand were used to calculate the K-factor using inherent soil parameters, as described by Dangler and El-Swaify (1976) for tropical soils. Soil structure was obtained by microscopic observation to establish the dominant shape of the grains while permeability (hydraulic conductivity) was determined by the constant head test method using a permeameter and associated components.

The following equation (*3.9*) was used to compute K using the values for the measured soil properties:

$$K = \frac{\left[2.1\times10^{-4}(12-MO)M^{1.14}+3.25(S-2)+2.5(P-3)\right]}{100} \qquad (3.9)$$

Where

K is the soil erodibility expressed in t.ha.hour/ha.MJ.mm in which t stands for tonnes, ha(hectare), MJ (mega joule) and mm(millimeter);

MO is percentage organic matter;

M is textural term for percentage of very fine sand plus percent silt;

S is the structure class code that varies from 1 to 4 where 1 is for fragmented structure and 4 for coarse structure.

P is the permeability code that varies from 1 to 6 (Ezzaouini *et al*., 2020).

3.10.4 Slope length and steepness, LS-factor

Topography and steepness (LS) accounting for runoff length and slope was calculated using the equation (*3.10*);

$$LS = \left(\frac{\lambda}{22.13}\right)^{m} x\ 65.4 \sin^2 \beta + 4.56 \sin \beta + 0.0654 \quad (3.10)$$

where;

LS is slope length

λ is the length of slope in m,

$\beta$is percent slope,

m = 0.5 if $\beta \geq 5\%$; m = 0.3 if $1<\beta<5\%$; m = 0.2 if $\beta \leq 1$

3.10.5 Cover management, C-factor

Cover management factor was estimated using vegetation cover conditions in the runoff plots. Sighting frame technology was employed to determine percentage of ground covered. Cover management factor (C factor) at any given time was calculated using equation (*3.11*).

$$C = exp\ (-0.06\ i) \quad (3.11)$$

Where;

C is the cover management factor

i is the intercepted energy and = mean cover.

3.10.6 Support practice P-factor

At the plot scale, there is no mechanical conservation measure. Therefore, P value was taken as 1.

3.11 Calibration and validation of MUSLE model

MUSLE model uses runoff factors to predict sediment yield unlike USLE and RUSLE which uses rainfall erosivity. The advantage of this model over other models available for analysis of soil erosion is that MUSLE requires a few variables and simple to use since it is an empirical model allowing researchers to input parameters manually.

3.11.1 Evaluation criteria

The performance of the model was evaluated using graphical comparisons and conducting various statistical tests including; Nash-Sutcliffe efficiency (NSE), Bias, coefficient of correlation (r), coefficient of determination (R^2) and Kling-Gupta Efficiency (KGE).

3.11.2 MUSLE model calibration

Sediment yields from the runoff plots were measured for two rainfall events in early stages of crop growth and used for calibration. Calibration was done by adjusting the Original runoff energy factors (α and β) and other MUSLE factors (K,LS,C and P) to suit Saimo catchment conditions.

3.11.3 MUSLE model validation

In validation, the remaining sediment yields from the other seven rainfall events were used.

3.11.4 MUSLE testing

The ability of the model to predict observed results were done using Nash-Sutcliffe efficiency (NSE), Coefficient of determination (R^2), Coefficient of correlation (r), Kling-Gupta efficiency (KGE), and percent BIAS (PBIAS). Krause *et al.*, (2005) used and recommended the listed hydrological model assessments.

3.11.5 Goodness of fit

NSE which depicts goodness of fit involves subtracting the absolute squared differences between the measured and the simulated values divided by the variance of measured values as provided in Equation (*3.12*).

$$NSE = 1 - \frac{\sum_{i=1}^{n}(M_i - S_i)^2}{\sum_{i=1}^{n}(M_i - \bar{M})^2} \quad (3.12)$$

where

M_i is the measured value,

S_i is the simulated value and

$\bar{M}$ is mean of measured values and n was the number of observations.

The NSE values vary from a negative value to 1. A value of 1 indicates a perfect fit whereas a negative value shows that the prediction of the model is worse than the average of the observed data.

Calibration of the model was also done using the bias method (BIAS) Equation (*3.13*), which entails minimization of the difference between measured values and the simulated sediments as used. Ezzaouini *et al*., (2020) in their study found the optimal value of BIAS to be 0.

$$BIAS = \frac{\sum_{i=1}^{n}(M_i - S_i)}{\sum_{i=1}^{n}(M_i)} \quad (3.13)$$

where

M_i is the measured value,

S_i is the simulated value and

n was the number of observations.

For model reliability the model was also calibrated using Kling-Gupta Efficiency (KGE) method (Ezzaouini *et al.*, 2020). Like NSE, KGE = 1 indicates perfect agreement between simulations and observations. Various authors use positive KGE values as indicative of 'good' model simulations, whereas negative KGE values are considered 'bad', without explicitly indicating that they treat KGE = 0 as their threshold between 'good' and 'bad' performance (Knoben *et al*., 2019).

$$KGE = 1 - \sqrt{(r-1)^2 + \left(\frac{\sigma_{sim}}{\sigma_{mea}} - 1\right)^2 + \left(\frac{\mu_{sim}}{\mu_{mea}} - 1\right)^2} \quad (3.14)$$

where

r is simple correlation coefficient between measured and observed sediments,

μ_{sim} is the mean of simulated sediments,

μ_{mea} is the mean of measured sediments,

σ_{sim} is the standard deviation of simulated sediments,

σ_{mea} is standard deviation of measured sediments and the optimal value of KGE is 1.

The coefficient of determination (R^2) is one of the frequently used criteria and was employed in this study. R^2 describes the proportion of the total variance in the measured data that can be explained by the model. It ranges from 0.0 to 1.0, with higher values indicating better agreement. It is given by Equation (*3.15*);

$$R^2 = \frac{\sum_{i=1}^{N}\left[O_i - O_{Avg}\right]\left[S_i - S_{Avg}\right]}{\left[\sum_{i=1}^{N}\left[(O_i - O_{Avg})^2\right]^{0.5}\sum_{i=1}^{N}\left[(S_i - S_{Avg})^2\right]^{0.5}\right]} \quad (3.15)$$

where

O_i is the measured value,

O_{Avg} is the mean of the measured values and N is the number of observations.

S_i is the simulated value and

S_{Avg} is the mean of the simulated values

The coefficient of correlation (r) is the square root of the coefficient of determination (R^2).

3.12 Sediment Yield Simulation

After calibration and validation, simulations were run in the model to predict sediment yields in different six scenarios of cover management and support practice factors (Table 3.1) that mimics the different land uses and the changes in the sediment yield generated in the Saimo Catchment.

Table 3.1: Cover and Support practice scenarios

Scenario	Cover management	Support practice
1	0.1	1.0
2	0.1	0.8
3	0.1	0.6
4	1	1.0
5	1	0.8
6	1	0.6

CHAPTER FOUR

RESULTS AND DISCUSSION

4.1 Introduction

This chapter presents various results based on the field data: soil texture, bulk density, organic carbon, organic matter, sieve analysis which are used to calculate soil erodibility factor. It also gives analysis on total runoff and peak runoff recorded per rainfall event. Further, slope length and steepness, cover management and support practices during the study period are also given in this chapter. MUSLE model calibration, validation and simulation as well as its interpretation and analysis of various results are outlined in this chapter.

4.2 Soil erodibility, slope length and steepness, cover management and support practice

4.2.1 Soil erodibility (K)

Soil erodibility which is a function of soil texture, organic matter, soil structure and permeability was determined in the preceding sub-sections. Soil erodibility factor was recorded as 0.18 as presented in appendix IV (table 4.4).

i) Soil texture, bulk density and percent organic matter

Random composite sampling method was used to collect soil samples within the research site where runoff plots were to be installed in a zig-zag pattern. Three points were selected and soil analysis is presented in table 4.1.

Table 4.1: Texture, Bulk Density, Organic Carbon and Organic Matter of Soil

Sample	Sand	Silt	Clay	Textural class	Bulk density (g/cm^3)	Organic carbon (%)	Organic matter (%)
PT1-1	54	34	12	Sandy loam	1.14	2.31	4.0
PT1-2	52	35	13	Loam	1.10	1.66	2.9
PT2-1	54	35	11	Sandy loam	1.01	2.53	4.4
PT2-2	51	35	14	Loam	1.04	1.88	3.2
PT3-1	55	35	10	Sandy loam	0.99	2.14	3.7
PT3-2	47	38	15	Loam	1.06	1.44	2.5
Mean	**52.2**	**35.3**	**12.5**	**Sandy loam**	**1.06**	**1.99**	**3.4**

From the six samples, the highest percentage of sand was 55% found in Point 3-1, the highest silt was found in PT3-2, and the highest clay was 15% found in PT2-2. The textural classes in the study area was sandy loam and loam. The means of sand, silt and clay in the area were 52.2%, 35.3% and 12.5%, respectively. The top soil in study area is sandy loam while the soil at 200 mm is loam. Taking the means, the soil texture is sandy loam (García-Gaines and Frankenstein, 2015). Soil texture is the main characteristic that affects soil erodibility and therefore with sandy loam and loam soil they are expected to be less erodible than silt or very fine sand (Bonilla *et al.*, 2012).

The bulk density of the soil ranged from 0.99 g/cm^3 to 1.14 g/cm^3 with a mean value of 1.06 g/cm^3. The mean bulk densities for top soil and bottom soil are 1.05g/cm^2 and 1.07 g/cm^3, respectively meaning that low bulk densities for the top soil. The mean bulk density of 1.06 g/cm^3 was close to 1.0 g/cm^3 observed at the depths of 0-19 cm observed in Romania. Low mean bulk densities are associated with low degree of compaction and consequently means that the soil is loose and can be susceptible to erosion (Moraru, *et al.,* 2020).

The percentage of organic carbon varied from 1.44% to 2.53%. The percentage of organic matter varied from 2.5% to 4.4%. The organic carbon falls within the agricultural soils under grain production that have soil organic carbon of between 0.8-2.0% found at depths of 0-10 cm and have bulk density of 1.0 g/cm^3. It can be noted that organic carbon is 58% of organic matter (Griffin, E, *et al.,* 2013).

ii) Sieve analysis

The percentage passing through different sieve sizes is shown in Figure4.1. The results were obtained from three sampling sites with two samples from each site. The percentage passing 0.1 mm sieve were all the same for the three sites. The percentage passing started to differ after 0.2 mm. This difference is very clear for sieve size 1 mm. The highest percentage 27.59 passing 1 mm sieve was observed in Pit 3 position 1 (PT31) while the lowest percentage of 10.46 was observed in Pit 1 position 1 (PT11). The same trend was observed in 2 mm sieve where it was found that the highest percentage passing was 41.7 observed in PT31 and the lowest was 25.92 observed in PT11. Samples from PT31, PT22 and PT21 had higher passing percentages than the mean while those that were lower than the mean were observed from PT11 and PT32. Samples from PT12 was the same as the mean but increased after 2mm sieve.

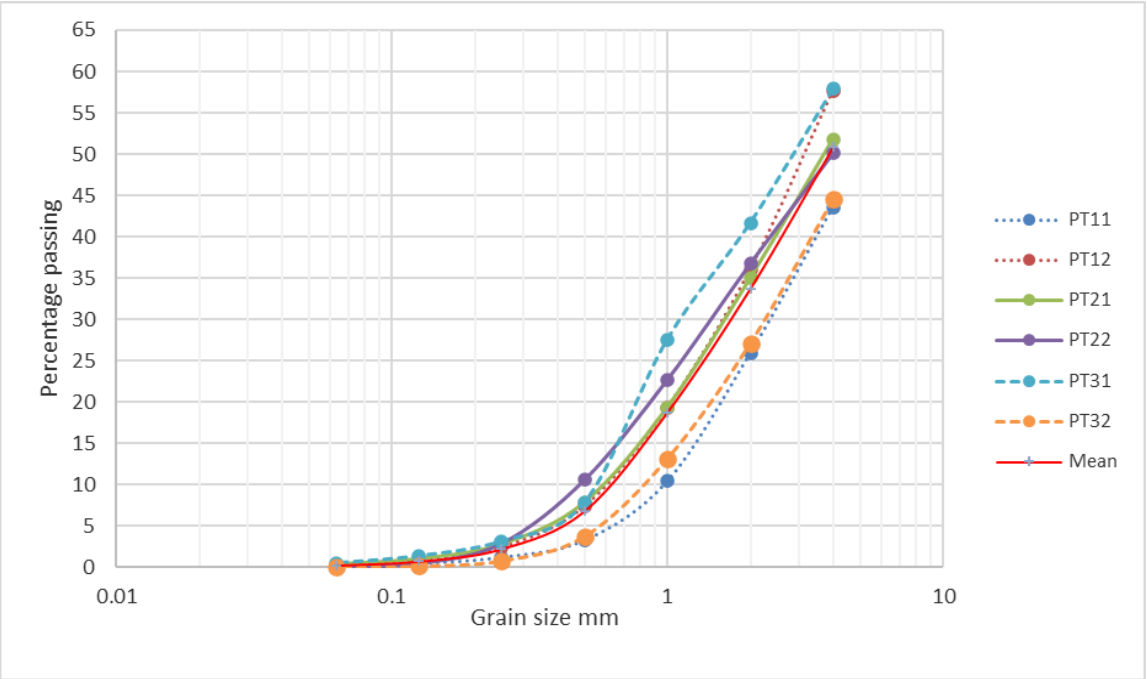

Figure 4.1: Percentage passing different sieves for soil samples in the study area

Based on the mean percentage passing, fine sand that is between 0.1 to 0.25 mm was found to be 1.75%. Therefore, the total value for fine sand and silt gives 37.1%.

High values of silt and fine sand increases the detachability of soil and hence increased splash erosion. These small particles are hard to aggregate and can easily be transported. Small particles like silt and fine sand are more erodible than large particles because of difference in inertial and drag forces (Sun, *et al.*, 2021).

iii) Saturated hydraulic conductivity

The saturated hydraulic conductivity varied from 8.0 µm/s to 41.3 µm/s with a mean value of 24.1 µm/s as shown in Table 4.2 below.

Table 4.2: Saturated Hydraulic Conductivity

Sample	Q(ml)	L (cm)	H (cm)	Area (cm^2)	Ksat µm/s	Ksat Class	Code
PT1-1	570	4	6	25.52	41.3	High	2
PT1-2	110	4	6	1.10	8.0	Moderately High	3
PT2-1	480	4	6	1.01	34.8	High	2
PT2-2	170	4	6	1.04	12.3	High	2
PT3-1	350	4	6	0.99	25.6	High	2
PT3-2	310	4	6	1.06	22.5	High	2
Mean					**24.1**	**High**	**2**

There were only two classes high and moderately high translating to code 2 and 3, respectively. High values of hydraulic conductivity indicate permeable material through which water can pass easily and therefore in Saimo catchment, the rate of water permeability ranges between moderately high and high.

Soils samples in PT2-2 had saturated hydraulic conductivity of 12.3 µm/s, which is close to the mean of sandy loam soils of 13.7 µm/s observed from a sample size of 2123 (García-Gutiérrez, *et al.,* 2018). Soils with higher clay content and aggregating particles, the packing and consequently the Ksat of these soils is not just mainly affected by the PSD, but also by aggregation, which cannot be accounted for in the IE value (García-Gutiérrez, *et al.,* 2018).

4.2.2 Slope length and steepness (LS)

The runoff length of the runoff plot measured 4.8 m as indicated in figure 3.3 (a). The slope of the research site was done by a line level and confirmed by clinometer to be 2%. Equation 3.10 was then used to calculate LS factor and a value of 0.173 obtained as recorded in appendix IV (table 4.3 and 4.4).

4.2.3 Cover management (C)

Bean crop grown subjected to both no mulching and mulching grew very well during the experiment and percentage cover was taken every time runoff is recorded and in the different stages of growth. Figure 4.2 presents bean crop during the study period.

Figure 4.2: Bean crop under Mulching, no mulch and control during the study period

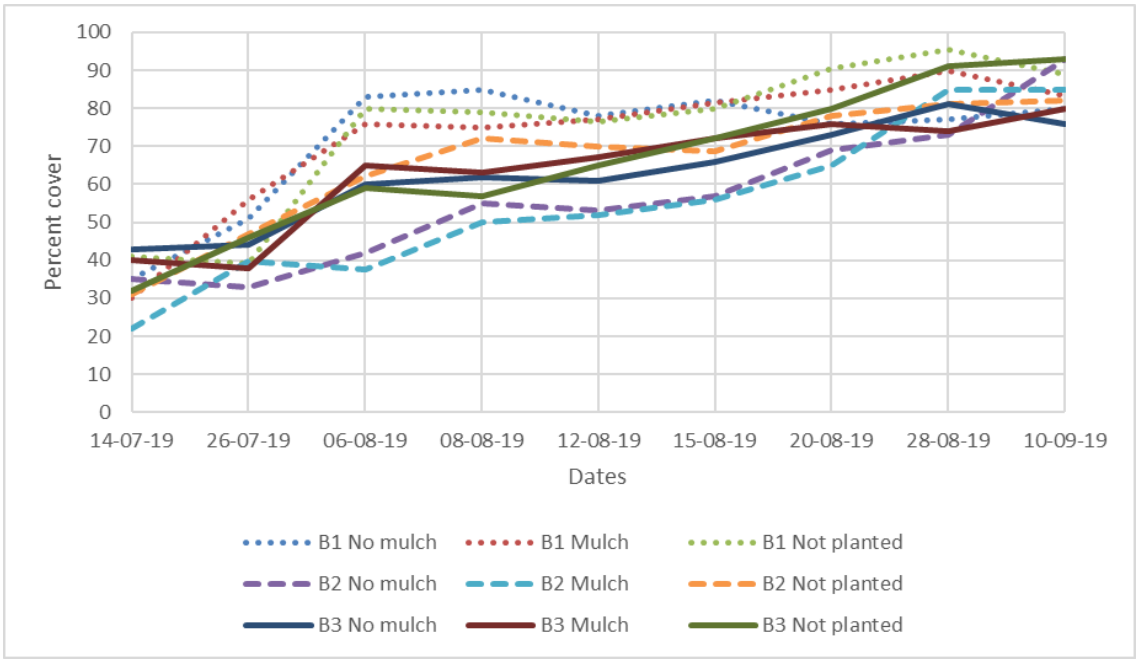

Figure 4. 3: Percentage cover for bean from July to September 2019

Block 1 had the highest percentage cover ranging from 40-95% for all the treatments from 26 July to 28 August. Block 2 under no mulch and mulch treatments had the lowest percent cover ranging from 32-75% for the same period. Block 2 with no planting had higher percentage cover above 47.5% compared with those with bean crop planted in the same block. Block 3 had intermediate percent cover ranging between 38-90% as seen in blocks 1 and 2 for the same period. Block 3 under no bean crop planted had the highest percent cover (93%) towards the end of the growing season.

4.2.4 Support practice (P)

There were no any support practices done at the runoff plots therefore a value of 1 was taken.

4.3 Rainfall intensities

The rainfall intensities during the research are shown in Figure 4.4. The rainfall intensities were used in calculation of peak runoff (q_p)and presented in table 4.3 below. Total runoff discharge (Q) resulting after every rainfall event was recorded and presented in appendix IV (table 4.3 and table 4.4).

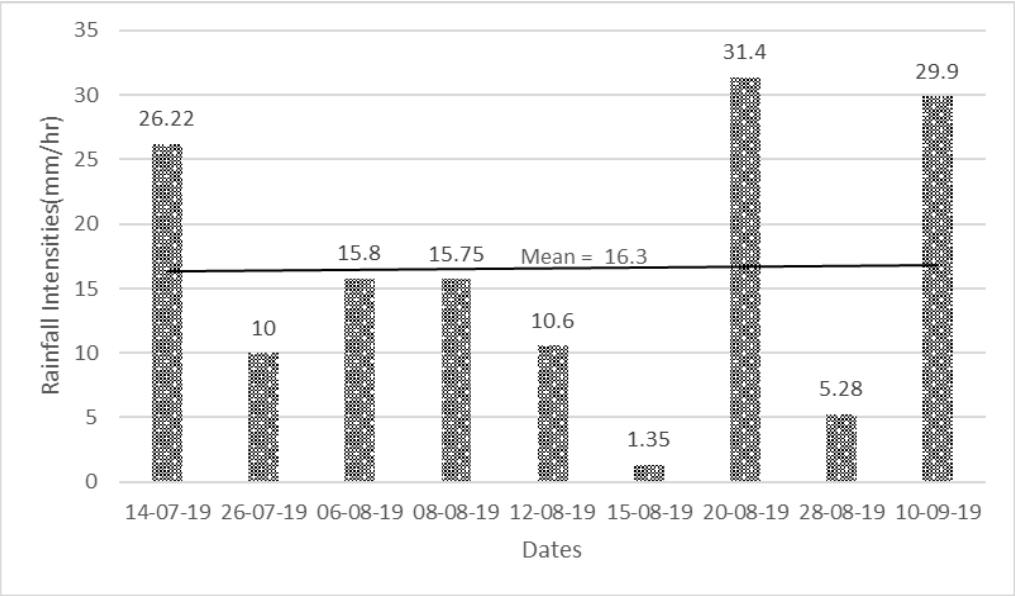

Figure 4.4: Rainfall Intensities during the study period

The highest and lowest rainfall intensities were 31.4 mm/hr and 1.35 mm/hr, respectively with a mean of 16.3 mm/hr. Only three events were more than the mean rainfall intensity obtained. The rainfall-runoff relationship for any rainstorm depends on the dynamic interaction between rain intensity, soil infiltration and surface storage. Runoff occurs whenever rain intensity exceeds the infiltration capacity of the soil, providing there are no physical obstructions to surface flow.

Table 4.3: Peak discharge in different plots on different dates

	Dates	Maximum peak discharges (litres/s)	Plots where peak was found	Measured sediments (g) in order of the plots	Maximum sediments (g) on each day	Maximum total volume of water (ml)	tons of soil loss per acre per year
1.	14-07-19	0.028	B1T3, B2T3, B3T3	111.2, 274.2, 302	302 (B3T3)	14210 (B3T3)	46.47
2.	26-07-19	0.011	B1T3, B2T3, B3T3	2.5, 12.0, 5.3	82.3 (B2T2)	1400 (B2T2)	12.66
3.	06-08-19	0.017	B1T3, B2T3, B3T3	2.50, 1.4, 3.5	14.0 (B2T2)	1750 (B3T3)	2.15
4.	09-08-19	0.017	B1T3, B2T3, B3T3	17.7, 37.6, 38.4	38.4 (B3T3)	12950(B3T2)	5.91
5.	12-08-19	0.011	B1T3, B2T3, B3T3	0.09, 0.8, 0.2	11.6 (B3T2)	1020(B3T3)	1.79
6.	15-08-19	0.001	B1T3, B2T3, B3T3	0.04, 0.02, 0.11	1.14 (B3T2)	710(B3T3)	0.18
7.	20-08-19	0.033	B1T3, B2T3, B3T3	0, 4.0, 35.6	35.6(B3T3)	13720 (B3T2)	5.48
8.	28-08-19	0.006	B1T3, B2T3, B3T3	0.05, 0.4, 0.54	3.9(B2T2)	2360 (B3T2)	0.60
9.	10-09-19	0.032	B1T3, B2T3, B3T3	2.4, 0, 0	58.5 (B2T2)	15250(B3T2)	9.00

From Table 4.3, it is clear that the maximum discharges occurred in plots that were not planted for all the blocks. The maximum sediments for the nine events had the highest value of 302 grams observed in control block 3 (B3T3). This maximum sediment load was attributed to best combination of the maximum peak discharge (q) and maximum total volume of water (Q) that was collected in Block 3 treatment 3 (B3T3) on 14th July 2019. The maximum total volume of water was collected mostly in block 3. This is the case for 8 out of 9 days where the observations were made.

The rainfall intensities were well below the extreme rainfalls of 1200 mm/hr used in a study in China. The soil erosion is therefore expected to be more during high rainfall intensities since soil erosion is directly proportional to raindrop (Sun, *et al.,* 2021). Hence high intensity rainfall of 31.4, 29.9 and 26.22 mm/hr resulted in higher sediment yields when compared to low intensity rainfall of 5.28 and 1.35 mm/hr which resulted in lower sediment yields.

The sediment yields in t/acre/year for rainfall events numbers 1, 2, 4, 7, 9 were 46.47, 12.66, 5.91, 5.48, and 9.00 respectively which is below the average tolerable soil loss threshold is 10 t/ha/y (Lufafa *et al., 2003*)

This could be attributed to high rainfall intensity and the level of soil cover during the study. However, for rainfall events 3, 5, 6 and 8 were within the tolerable limit.

4.4 Analysis of Variance (ANOVA) of the Control Plots

Table 4.4 below show the sediment yields in control blocks.

Table 4.4: Observed sediment yields in the control blocks

		Observed sediment yields in the control plots (g)			
Date	**Rainfall intensity (mm/h)**	**Block 1**	**Block 2**	**Block 3**	**TOTAL**
14/7/19	26.22	111.2	274.2	301.9	**687.3**
26/7/19	10.00	2.53	11.95	5.28	**19.76**
06/8/19	15.08	2.53	1.43	3.53	**7.49**
15/8/19	1.35	0.04	0.02	0.11	**0.17**
	TOTAL	**116.3**	**287.6**	**310.82**	**714.72**

For the control plots, there are no repetitions and no interactions between the treatments.

$C_T = (\sum_i^a \sum_j^b \sum_k^c y_{ijk})^2 = \frac{y_{...}^2}{abn}$ where a=4, b=3 and n=1

$$= \frac{714.72^2}{4 \times 3 \times 1} = 42,568.7$$

$$SS_T = \sum_i^a \sum_j^b \sum_k^n y_{ijk}^2 - CT$$

$$= 111.2^2 + 274.2^2 + ... + 0.02^2 + 0.11^2 - 42,568.7 = 136,324.0$$

$SS_A = \sum_{i=1}^a \frac{y_{i..}^2}{bn} - CT$

$$= \frac{687.3^2 + 19.76^2 + 7.49^2 + 0.17^2}{3 \times 1} - 42,568.7 = 115,040.6$$

$SS_B = \sum_{j=1}^b \frac{y_{.j.}^2}{an} - CT$ $= \frac{116.3^2 + 287.6^2 + 310.82^2}{4 \times 1} - 42,568.7 = 5,643.4$

$SS_E = SS_T - SS_A - SS_B$ $= 136,324.0 - 115,040.6 - 5,643.4 = 15,640$

Table 4.5: Analysis of variance

Source of variation	SS	DF	MS	Fob	p-value
Treatment A (Rainfall intensity, mm/h)	SS_A = 115,040.6	(a-1) = 4-1 = 3	SS_A/(a-1) =115,040.6/3 = 38,346.9	MS_A/MS_E = 14.71	$F_{crit} = F_{(3,6)0.05}$ = 4.76
Block B (Runoff plots)	SS_B = 5,643.4	(b-1) =3-1 = 2	SS_B/(b-1) =5,643.4/2 = 2,821.7	MS_B/MS_E = 1.08	$F_{crit} = F_{(2,6)0.05}$ = 5.14
Error	SS_E = 15,640	(a-1) (b-1) = 6	SS_E/ (a-1) (b-1) =15,640/6 = 2,606.7		
Total	**136,324.0**				

$F_{obs} > F_{crit}$ for rainfall intensity in runoff plots i.e., 14.71 > 4.76.

We reject the null hypothesis that $H0_1$: $\mu_{Treatment1} = \mu_{Treatment2} = \mu_{Treatment3} = \mu_{Treatment4} = 0$ and conclude that rainfall intensity affects the sediment yields in the runoff plots.

$F_{obs} < F_{crit}$ for homogeneity in runoff plots i.e., 1.08 < 5.14.

We accept the null hypothesis that $H0_1$: $\mu_{Block1} = \mu_{Block2} = \mu_{Block3} = 0$ and conclude that there is no evidence to suggest that the soil homogeneity in the runoff plots affect the sediment yields.

Hence,

- The rainfall intensity in the runoff plots within the Tugen hills do not produce the same sediment yields during a rainfall event (do not have the same population means).
- The soils in the runoff plots (Blocks) are homogenous i.e., the physical and chemical properties that includes bulk density, soil texture, percent Organic Matter (% OM) and percent Organic Carbon (% OC) do not play a significant role in sediment yield production in the Tugen hills.

4.5 Calibration and validation of MUSLE model

4.5.1 Model Calibration

Data collected from two events at the beginning of the study were used in model calibration. The rainfall intensities for the events were 26.2 and 10mm/h respectively. The measured and simulated sediments for each plot for the two rainfall events are shown in Figures 4.4 and 4.5.

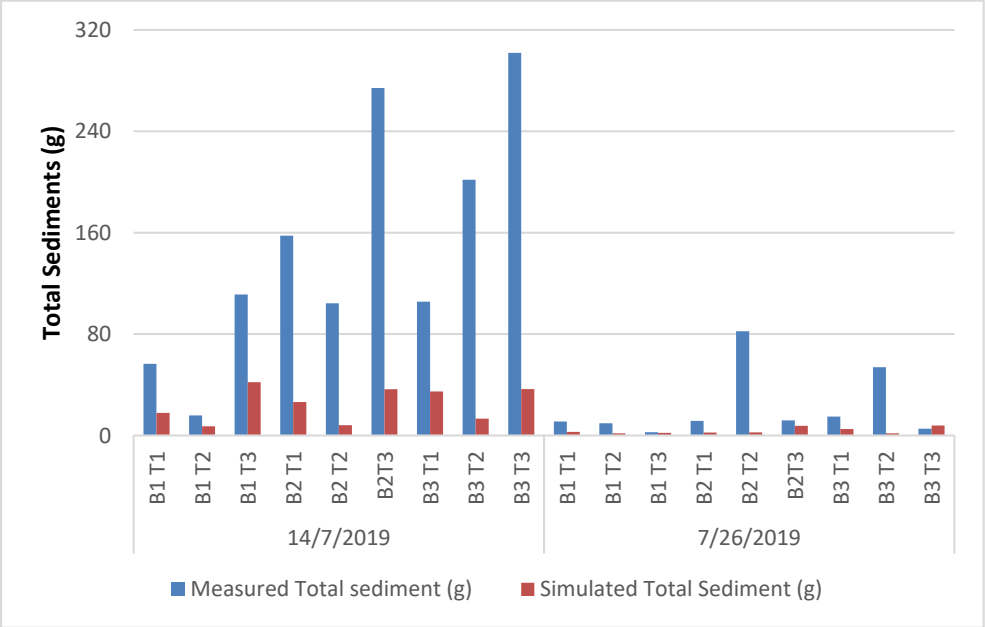

Figure 4.4: Calibration results for the Site

Figure 4.4 shows that the higher intensity rainfall event of 26.22 mm/h and peak discharge (q_p) of 0.028 l/s on 14/07/2019 resulted in higher measured total sediments when compared with the low intensity rainfall event of 10.0 mm/h on 26/07/2019 which resulted in lower measured total sediments. In the MUSLE equation, q_p is associated with sediment transportation hence the lower value of 0.011 l/s meant that less sediments were able to reach the runoff plot outlet as simulated (Fig 4.4).

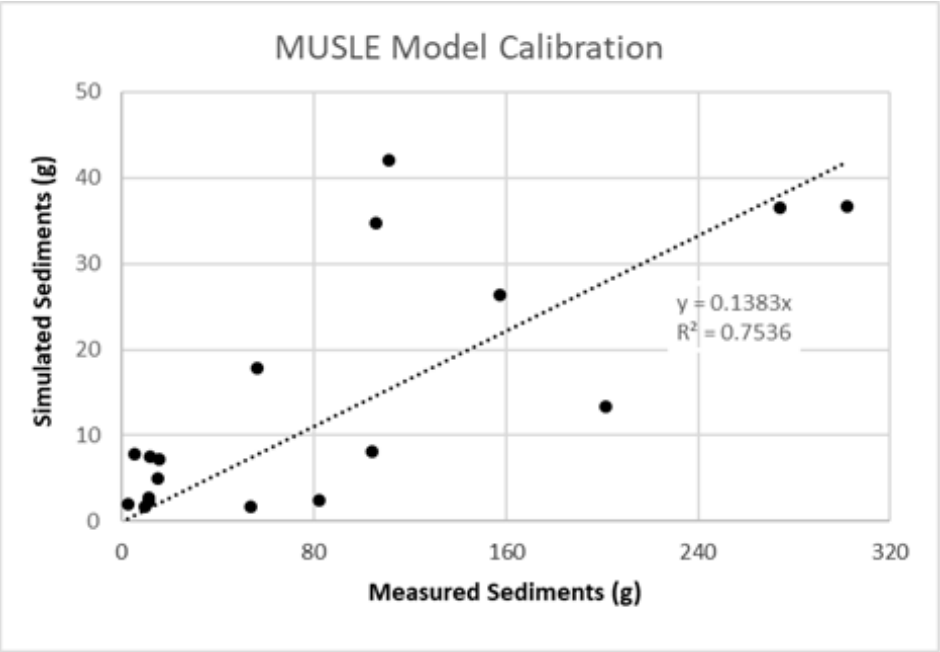

Figure 4.5: Calibration of MUSLE model for sediment yields

The observed and simulated data were positively correlated as shown by the values of coefficient of correlation, r of 0.87 and coefficient of determination, R^2 of 0.75. The MUSLE model was able to simulate satisfactorily much higher sediments loads for higher rainfall intensities and lower sediments for lower rainfall intensities (Figure 4.5).

4.5.2 Model Validation

Seven events were used to validate the model. Figure 4.6 shows that high rainfall intensities of 31.4 mm/h and 29.9 mm/h resulted in peak runoffs of 0.033 l/s and 0.0199 l/s and yielded sediments of 70.19g and 70.15g respectively.

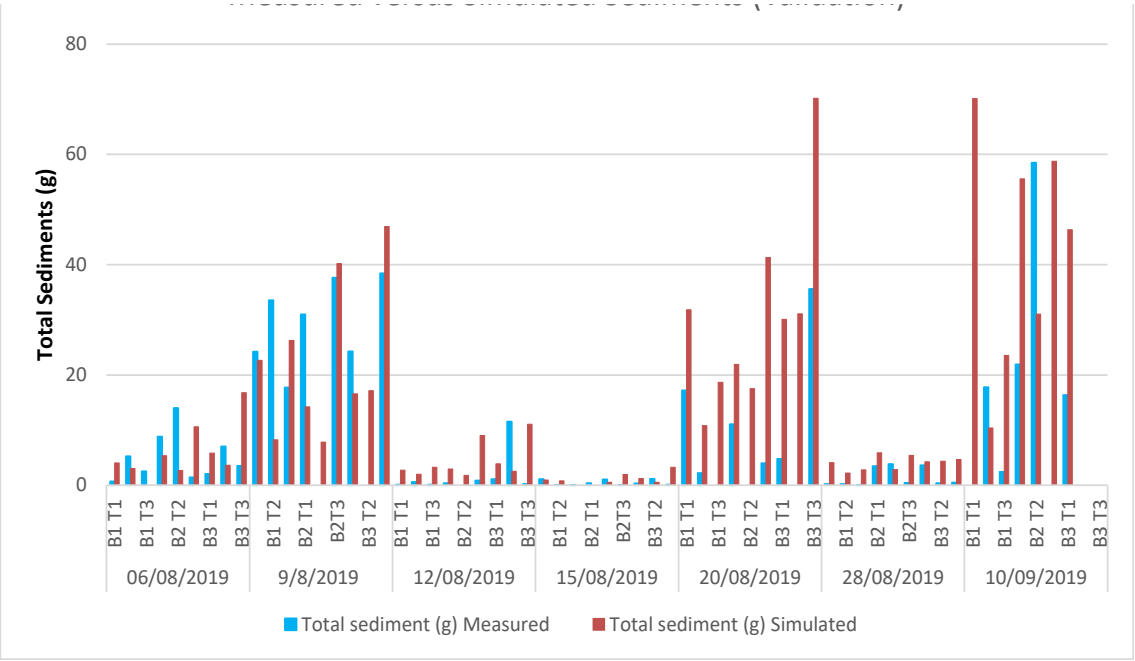

Figure 4.6 Validation Results for the Site

Low rainfall intensities of 1.35 mm/h and 5.28 mm/h generated a runoff of 0.00144 l/s and 0.00352 l/s resulting in maximum sediment yield of 3.26g and 5.87g respectively. In MUSLE model, high rainfall intensities translate to generation of high runoff resulting to large amounts of sediments. This means high rainfall intensity possesses high energy which leads to high detachability of soil particles. Likewise, high runoff rates increase the speed at which particles are entrained along the surface thereby causing further detachment of soil particles and transportation downslope resulting in generation of more sediments.

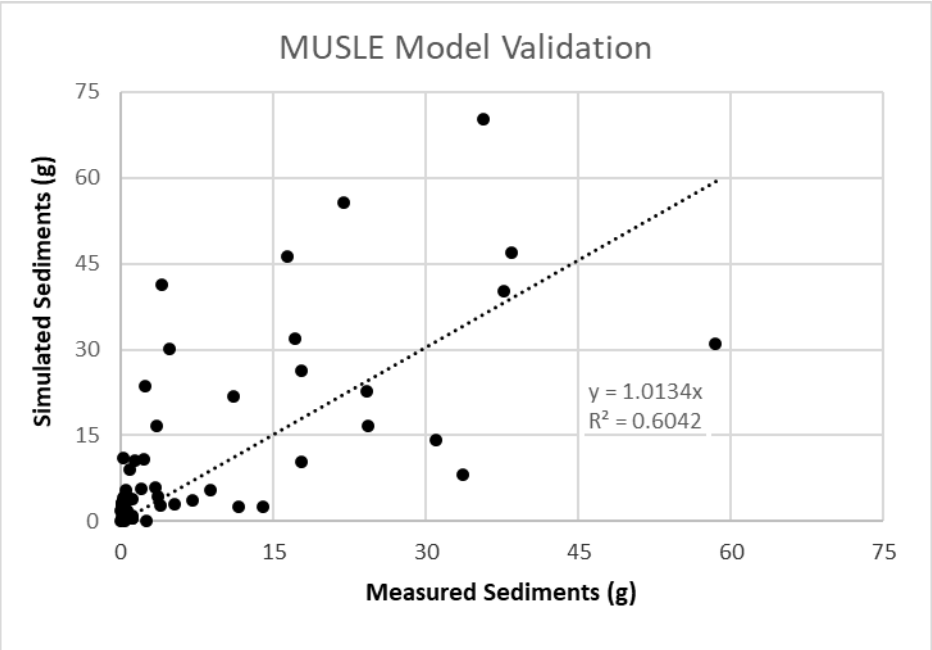

Figure 4.7: MUSLE Model Validation

The observed and simulated data were positively correlated as shown by the value of coefficient of correlation, r of 0.78 and coefficient of determination, R^2 of 0.60. The model was able to simulate satisfactorily much higher sediments for higher rainfall intensities and lower sediments for lower rainfall intensities (Figure 4.7).

i) Model Simulations

Model simulations of rainfall intensity against sediment yield for blocks 1, 2 and 3 were run for no mulch, mulch and not planted treatments. The results and discussions are presented in figures 4.8, 4.9 and 4.10.

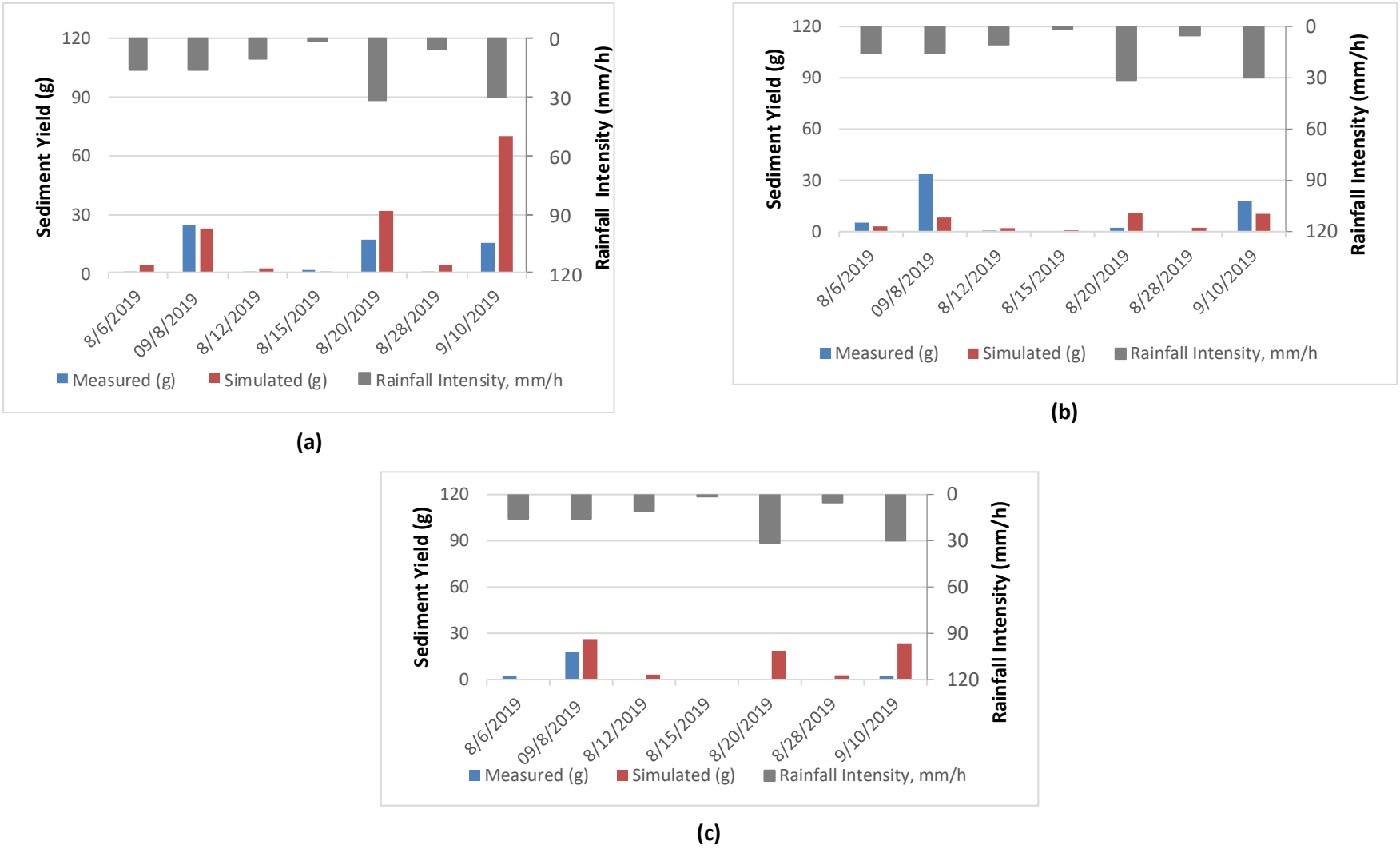

Figure 4.8: Model simulations for Block 1 (a) No mulch, (b) Mulch and (c) Not Planted

In block 1, rainfall intensity of 29.9 mm/h simulated sediments measuring 70.15g, 10.37g and 23.53g in no mulch, mulch and not planted plots respectively. The high amount of sediments generated in no mulch plot can be attributed to disturbance of soil by mechanical weeding which took place on 9/9/2019 whereas the minimum sediments generated in mulched plot is attributed to the no disturbance of soil as there were very minimal weeds.

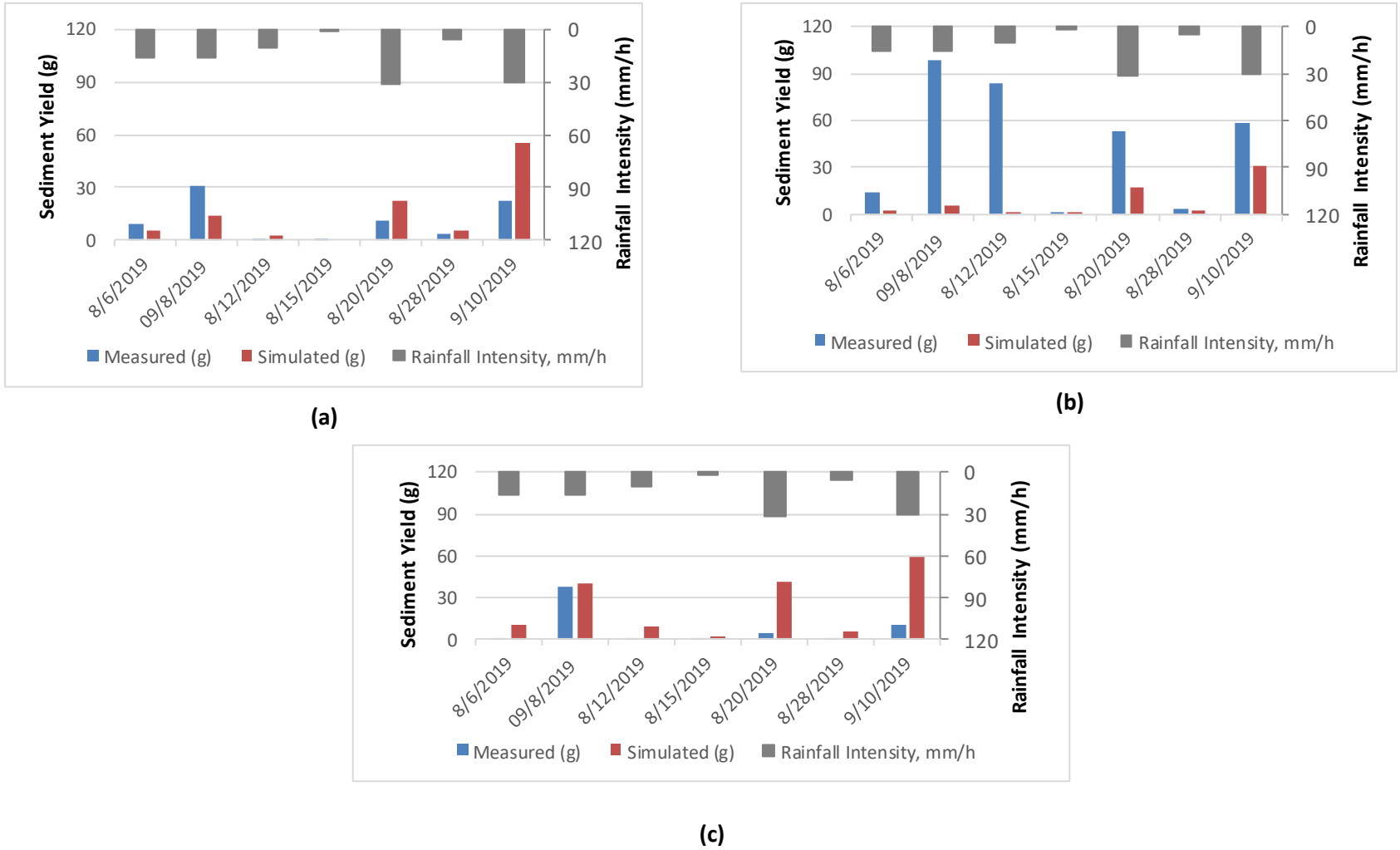

Figure 4.9: Model simulations for Block 2 (a) No mulch, (b) Mulch and (c) Not Planted

In block 2, the model under estimated sediments in mulch plot for all the 6 days. The highest difference between observed and simulated values were 93.23g which occurred on 9/8/2019 with rainfall intensity of 15.75 mm/h followed by a difference of 81.91g recorded on12/8/2019 with rainfall intensity of 10.60 mm/h. In the plot not planted, the model predicted high amounts of sediments than those observed in all the 6 days. The highest value simulated was 58.76g while the lowest was 1.95g under rainfall intensities of 29.9 mm/h and 1.35 mm/h respectively.

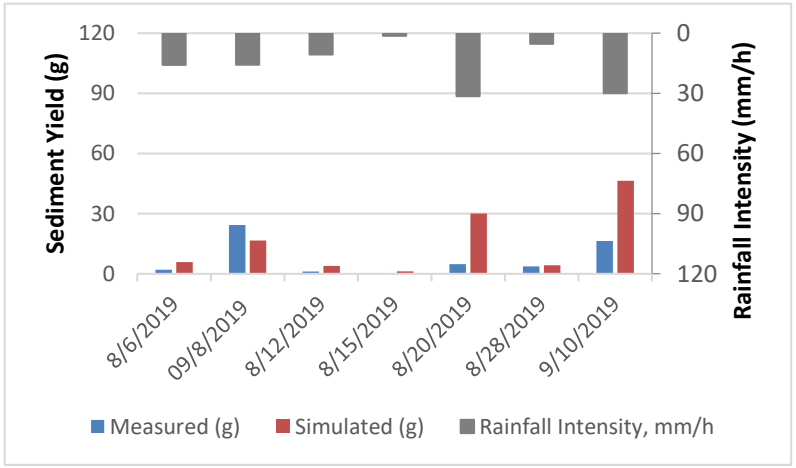

(a)

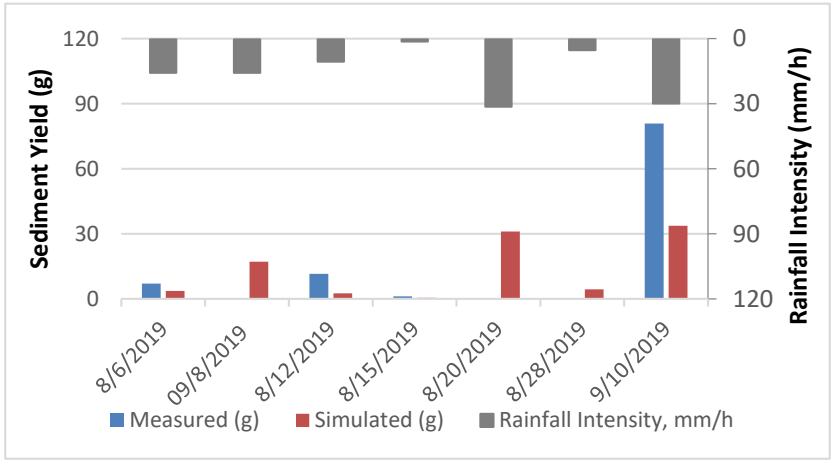

(b)

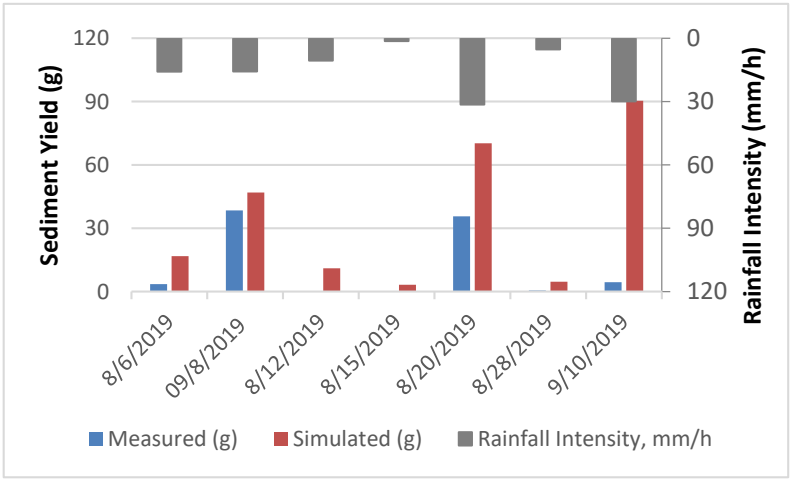

(c)

Figure 4.10: Model simulations for Block 3 (a) No mulch, (b) Mulch and (c) Not Planted

In block 3, low sediments of 0.53g were observed on mulch plot with a rainfall intensity of 1.35 mm/h. The highest sediments predicted were on not planted plot with a value of 90.39g resulting from a rainfall intensity of 29.9 mm/h. Though plot not planted had highest percent cover, high amount of sediments generated may be attributed to the leaves for weeds not intercepting rain drops as compared to the leaves of the beans.

Phase	**α**	**β**	**PBIAS**	**KGE**	**R^2**	**r**	**NSE**
Calibration	11.8	0.546	0.83	-0.2	0.75	0.87	-0.40
Validation	11.8	0.546	-0.44	0.5	0.60	0.78	0.96
Required						-1 to 1	-∞<NSE<1.00

The α and β values were kept constant for all the days of the experiment. The value for β is site specific and for Saimo catchment it was determined during calibration as 0.546. There were some negative values of percent bias (PBIAS), Kling-Gupta Efficiency (KGE) and Nash-Sutcliffe efficiency (NSE). Though the PBIAS was 0.83 during calibration it was -0.44 during the validation phase. KGE and NSE were -0.20 and -0.40 respectively during calibration. R^2 and r values for calibration and validation were 0.75 and 0.87, and 0.60 and 0.78 respectively. This confirmed that the model performed well for both scenarios. The NSE value for validation was 0.96, further supporting the good performance of the model during validation.

The PBIAS measures the average tendency of the simulated values to be larger or smaller than their observed ones. Since PBIAS is expected to equal 0, then low magnitude indicates accurate model simulation. Positive (+ve) PBIAS indicates under-estimation bias while negative (-ve) PBIAS shows over-estimation. The Saimo catchment had lower values for both calibration and validation, showing accurate model simulations. The negative BIAS of -0.44 was within the same range as was observed in Morocco though the highest negative value there was -0.23.

A traditional metric used in hydrology to summarize model performance is the Nash-Sutcliffe Efficiency (NSE). Increasingly an alternative metric, the Kling-Gupta Efficiency (KGE), is used instead. When NSE is used, NSE = 0 corresponds to using the mean flow as a benchmark predictor. The same reasoning is applied in various

studies that use KGE as a metric: negative KGE values are often viewed in the literature as bad model performance and positive values are seen as good model performance. Knoben *et al.* (2019) showed that using the mean flow as a predictor does not result in KGE = 0, but instead KGE approx. 0.41. Thus, KGE values greater than -0.41 indicate that a model improves upon the mean flow benchmark even if the model's KGE value is negative. NSE and KGE values cannot be directly compared, because their relationship is non-unique and depends in part on the coefficient of variation of the observed time series. According to Knoben *et al.* (2019) the model simulations with values between -0.41<KGE<1 can be termed as reasonable model performance.

Modelers must take care not to let their interpretation of KGE values be (subconsciously) guided by their understanding of NSE values, because these two metrics cannot be compared in a straightforward manner. Instead of relying on the overall KGE value, in-depth analysis of the KGE components can allow a modeler to both better understand what the overall value means in terms of model errors and to modify the metric through weighting of the components to better align with the study's purpose.

4.6 Sediment Yield Simulation

Scenario analysis results was done using the maximum peak flow observed in the site. The permeability code, structure code and LS factor were taken as 2, 3.5 and 0.091, respectively. Table 4.5 shows Sediment Yields for different scenarios

Table 4.6: Sediment Yields for different scenarios

Scenario	Cover practice, C	Support, P	Sediment in g
1	0.1	1.0	11.7
2	0.1	0.8	9.41
3	0.1	0.6	7.06
4	1	1.0	117.6
5	1	0.8	94.1
6	1	0.6	70.6

The highest sediment of 117.6 g was observed under cover management of 1 and support practice of 1. The minimum was 7.06 g observed under cover management of 0.1 and cover practice of 0.6. The mean was 51.76 g. The model underestimated the results which is not the same as overestimation which was observed in Morocco by Ezzaouini *et al.*, (2020).

CHAPTER FIVE

CONCLUSIONS AND RECOMMENDATIONS

5.1 Conclusions

During the study, the parameters used in Modified Universal Soil Loss Equation (MUSLE) model were determined from field experiments and the following conclusions are drawn.

1. The soil within the study area were found to have mean bulk density of 1.06 g/cm^3. The total value for fine sand and silt gives 37.1%. with mean saturated hydraulic conductivity of 24.1 µm/s indicating that the soils within the experimental site were having high susceptibility to erosion. Overall, in the study area, the soil erodibility was found to be 0.18 whereas the slope and steepness factor being 0.173. The percent cover varied from a small value of 22% to a high value of 95% during the research period
2. Rainfall intensity and the degree of soil cover were found to influence sediment yields. For similar rainfall intensity, study plots with lower percentage cover experienced higher sediment yields to an upward of 104.17 tons/ha/year which is above the maximum tolerable limit of 10 tons/ha/year.
3. Under various land cover conditions, the relative sequences and orders of magnitude of runoff from the plots were reasonably simulated. Furthermore, the regression statistics and the NSE showed that the correlations between observed and simulated runoff amounts were reasonably good.
4. The MUSLE model is suitable in the modeling of sediment output under a given runoff volume and peak discharge from catchments under varied cover and with various management strategies, according to the findings of this study

5.2 Recommendations

Model calibration in this study was limited to the homogeneous circumstances of a small experimental plot setting and MUSLE was designed for a micro-watershed level, it is recommended that;

(i) The impact of the LS factor on event-based sediment yield be examined further on a broader scale.

(ii) Further studies be undertaken under virgin/uncultivated land within Saimo catchment and the results compared to the finding of this paper for better planning and management of the catchment.

(iii) The model can be used to assess sediment yield under various land management regimes and to plan environmental management, particularly in high-slope watersheds.

REFERENCES

Al-Smadi, M. A. (2007). Areal Modeling of Erosion for Environmental Nonpoint Applications (AMEENA) (Doctoral dissertation, Virginia Tech).

Alufah, S., Shisanya, C. A., & Obando, J. A. (2012). Analysis of factors influencing adoption of soil and water conservation technologies in Ngaciuma sub-catchment, Kenya. *African Journal of Basic & Applied Sciences, 4(5), 172-185*.

Angima, S. D., Stott, D. E., O'neill, M. K., Ong, C. K., & Weesies, G. A. (2003). Soil erosion prediction using RUSLE for central Kenyan highland conditions. Agriculture, ecosystems & environment, 97(1), 295-308.

Arekhi, S., Shabani, A., & Alavipanah, S. K. (2011). Evaluation of integrated KW-GIUH and MUSLE models to predict sediment yield using geographic information system (GIS) (Case study: Kengir watershed, Iran). *African Journal of Agricultural Research, 6(18), 4185-4198.*

Assaye, A. E. (2020). Farmers' perception on Soil Erosion and Adoption of Soil Conservation Measures in Ethiopia. *International Journal of Forest, Soil & Erosion, 10(1).*

Bai, Z. G., & Dent, D. L. (2006). Global assessment of land degradation and improvement: pilot study in Kenya.

Balasubramanian, A. (2017). Soil erosion–causes and effects. Centre for Advanced Studies in Earth Science, University of Mysore, Mysore.

Benavidez, R., Jackson, B., Maxwell, D., & Norton, K. (2018). A review of the (Revised) Universal Soil Loss Equation ((R) USLE): With a view to increasing its global applicability and improving soil loss estimates. *Hydrology and Earth System Sciences, 22(11), 6059-6086.*

Bonilla, C. A., & Johnson, O. I. (2012). Soil erodibility mapping and its correlation with soil properties in Central Chile. Geoderma, 189, 116-123.

Boongaling, C. G. K., Faustino-Eslava, D. V., & Lansigan, F. P. (2018). Modeling land use change impacts on hydrology and the use of landscape metrics as tools for watershed management: The case of an ungauged catchment in the Philippines. Land use policy, 72, 116-128

Borrelli, P., Robinson, D. A., Fleischer, L. R., Lugato, E., Ballabio, C., Alewell, C., ... & Panagos, P. (2017). An assessment of the global impact of 21st century land use change on soil erosion. Nature communications, 8(1), 1-13.

Camarasa-Belmonte, A. M., & Soriano, J. (2014). Empirical study of extreme rainfall intensity in a semi-arid environment at different time scales. Journal of Arid Environments, 100, 63-71.

Carvalho, F. P. (2017). Pesticides, environment, and food safety. Food and energy security, 6(2), 48-60.

Chalise, D., Kumar, L., Sharma, R., & Kristiansen, P. (2020). Assessing the impacts of tillage and mulch on soil erosion and corn yield. Agronomy, 10(1), 63.

Chuenchum, P., Xu, M., & Tang, W. (2019). Estimation of soil erosion and sediment yield in the Lancang–Mekong river using the modified revised universal soil loss equation and GIS techniques. Water, 12(1), 135.

Cook, R. D., & Weisberg, S. (1982). Residuals and influence in regression. New York: Chapman and Hall.

Dangler, E. W., & El-Swaify, S. A. (1976). Erosion of selected Hawaii soils by simulated rainfall. *Soil Science Society of America Journal, 40(5), 769-773.*

Dinka, M. O. (2020). Quantification of soil erosion and sediment yield for ungauged catchment using the RUSLE model: Case study for Lake Basaka catchment in Ethiopia. Lakes & Reservoirs: Research & Management, 25(2), 183-195.

Djoukbala, O., Hasbaia, M., Benselama, O., & Mazour, M. (2019). Comparison of the erosion prediction models from USLE, MUSLE and RUSLE in a Mediterranean watershed, case of Wadi Gazouana (NW of Algeria). Modeling Earth Systems and Environment, 5(2), 725-743.

Douglas, I. (2020). Urban geomorphology. In The Routledge Handbook of Urban Ecology (pp. 186-209). Routledge.

Duan, Y., Andrychowicz, M., Stadie, B., Jonathan Ho, O., Schneider, J., Sutskever, I., ... & Zaremba, W. (2017). One-shot imitation learning. Advances in neural information processing systems, 30.

Ezzaouini, M. A., Mahé, G., Kacimi, I., & Zerouali, A. (2020). Comparison of the MUSLE model and two years of solid transport measurement, in the Bouregreg Basin, and impact on the sedimentation in the Sidi Mohamed Ben Abdellah Reservoir, Morocco. *Water*, *12*(7), 1882.

García-Gaines, R. A., & Frankenstein, S. (2015). USCS and the USDA soil classification system: Development of a mapping scheme.

Griffin, E, Hoyle, FC & Murphy, DV (2013), 'Soil organic carbon', in Report card on sustainable natural resource use in Agriculture, Department of Agriculture and Food, Western Australia, viewed 16 May 2022, https://www.agric.wa.gov.au/sites/gateway/files/2.4%20Soil%20organic%20carbon.pdf

Gwapedza, D., Nyamela, N., Hughes, D. A., Slaughter, A. R., Mantel, S. K., & van der Waal, B. (2021). Prediction of sediment yield of the Inxu River catchment (South Africa) using the MUSLE. International Soil and Water Conservation Research, 9(1), 37-48.

Hayes, W. A. (2018). Conservation tillage systems and equipment requirements. In A Systems Approach to Conservation Tillage (pp. 21-40). CRC Press.

Hould-Gosselin, G., Rousseau, A. N., Gumiere, S. J., Hallema, D. W., Ratté-Fortin, C., Thériault, G., & Van Bochove, E. (2016). Modeling the sediment yield and the impact of vegetated filters using an event-based soil erosion model—a case study of a small Canadian watershed. Hydrological Processes, 30(16), 2835-2850.

Husic, A., Fox, J., Mahoney, T., Gerlitz, M., Pollock, E., & Backus, J. (2020). Optimal transport for assessing nitrate source-pathway connectivity. Water Resources Research, 56(10), e2020WR027446.

Jane, M. (2009). A review of constraints to ware Irish potatoes production in Kenya. Journal of horticulture and forestry, 1(7), 98-102.

Johansson, J., & Svensson, J. (2002). Land Degradation in the Semi-Arid Catchment of Lake Baringo, Kenya-a minor field study of physical causes with-a socioeconomic aspect.

Johnson, L. C. (1987). Soil loss tolerance: fact or myth?. Journal of soil and water conservation, 42(3), 155-160.

Karuku, G. N. (2018). Soil and water conservation measures and challenges in Kenya; A review.

Kebut, D. K. (2019). Assessment of Soil Erosion Dynamics Using Geospatial Technology Case Study of Lake Baringo Catchment (Doctoral dissertation, University of Nairobi).

Kimani, E. W., Ogendi, G. M., & Makenzi, P. M. (2014). An evaluation of constraints in climate change indigenous coping and adaptation strategies for sustainable agro-pastoral based livelihoods in Baringo County, Kenya. IOSR Journal of Environmental Science, Toxicology and Food Technology (IOSRJESTFT), 8(8), 38-58.

Knoben, W. J., Freer, J. E., & Woods, R. A. (2019). Inherent benchmark or not? Comparing Nash–Sutcliffe and Kling–Gupta efficiency scores. Hydrology and Earth System Sciences, 23(10), 4323-4331.

Kollongei, K. J., & Lorentz, S. A. (2015). Modelling hydrological processes, crop yields and NPS pollution in a small sub-tropical catchment in South Africa using ACRU-NPS. *Hydrological Sciences Journal, 60(11), 2003-2028.*

Kouli, M., Soupios, P., & Vallianatos, F. (2009). Soil erosion prediction using the revised universal soil loss equation (RUSLE) in a GIS framework, Chania, Northwestern Crete, Greece. Environmental geology, 57(3), 483-497.

Krause, P., Boyle, D. P., & Bäse, F. (2005). Comparison of different efficiency criteria for hydrological model assessment. Advances in geosciences, 5, 89-97.

Kumar, R., Mishra, J. S., Upadhyay, P. K., & Hans, H. (2019). Rice fallows in the Eastern India: problems and prospects. Indian J Agric Sci, 89(4), 567-77.

Lal, R. (2017). Soil erosion by wind and water: problems and prospects. In Soil erosion research methods (pp. 1-10). Routledge.

Licht, M. A., & Al-Kaisi, M. (2005). Strip-tillage effect on seedbed soil temperature and other soil physical properties. Soil and Tillage research, 80(1-2), 233-249.

Lin, S., Hernandez-Ramirez, G., Kryzanowski, L., Wallace, T., Grant, R., Degenhardt, R., ... & Powers, L. A. (2017). Timing of manure injection and nitrification inhibitors impacts on nitrous oxide emissions and nitrogen transformations in a barley crop. *Soil Science Society of America Journal, 81(6), 1595-1605.*

Lorentz, S. A., & Schulze, R. E. (1995). Sediment yield. Hydrology and agrohydrology: a text to accompany the ACRU, 3.

Lufafa, A., Tenywa, M. M., Isabirye, M., Majaliwa, M. J. G., & Woomer, P. L. (2003). Prediction of soil erosion in a Lake Victoria basin catchment using a GIS-based Universal Soil Loss model. Agricultural systems, 76(3), 883-894.

Lussier, J. M., Krzic, M., Smukler, S. M., Neufeld, K. R., Chizen, C. J., & Bomke, A. A. (2020). Labile soil carbon fractions as indicators of soil quality improvement under short-term grassland set-aside. Soil research, 58(4), 364-370.

Magdoff, F., & van Es, H. (2021). Building Soils for Better Crops. Ecological Management for Healthy Soils. Sustainable Agriculture Research and Education (SARE).

Mati, B. M., & Veihe, A. (2001). Application of the USLE in a savannah environment: comparative experiences from East and West Africa. *Singapore Journal of Tropical Geography, 22(2), 138-155.*

Mbaabu, P. R., Olago, D., Gichaba, M., Eckert, S., Eschen, R., Oriaso, S., ... & Schaffner, U. (2020). Restoration of degraded grasslands, but not invasion by Prosopis juliflora, avoids trade-offs between climate change mitigation and other ecosystem services. Scientific reports, 10(1), 1-13.

Moraru, S. S., Ene, A., & Badila, A. (2020). Physical and Hydro-Physical Characteristics of Soil in the Context of Climate Change. A Case Study in Danube River Basin, SE Romania. Sustainability, 12(21), 9174.

Morgan, R. P. C. (2009). Soil erosion and conservation. John Wiley & Sons.

Mudamburi, B. (2017). A comparison of the performance of Namibia-Specific Conservation and Conventional tillage technologies as used for pearl millet production in Northern Namibia (Doctoral dissertation, University of Namibia).

Mulinge, W., Gicheru, P., Murithi, F., Maingi, P., Kihiu, E., Kirui, O. K., & Mirzabaev, A. (2016). Economics of land degradation and improvement in Kenya. In Economics of land degradation and improvement–A global assessment for sustainable development (pp. 471-498). Springer, Cham.

Narantsogt, N., & Mohrlok, U. (2019). Evaluation of MAR methods for semi-arid, cold regions. Water, 11(12), 2548.

Nasidai, M. K. (2015). Calibration of a multi-factor weather index to determine the trigger event of claim payments on crop micro insurance in Eastern Kenya.

Niziolomski, J. C., Simmons, R. W., Rickson, R. J., & Hann, M. J. (2020). Efficacy of mulch and tillage options to reduce runoff and soil loss from asparagus interrows. Catena, 191, 104557.

Nwokoro, C. V., & Chima, F. O. (2017). Impact of environmental degradation on agricultural production and poverty in rural Nigeria. Am Int J Contemp Res, 7, 6-14.

Obando J.A., (2004). Catchment modelling for planning use of land and water resources in semiarid areas

Odada E. O, Onyando J. O and Obudho P. A. (2006). Lake Baringo: Addressing threatened biodiversity and livelihoods. Lakes & Reservoirs: Research and Management, 11: 287–299Doi: 10.1111/j.1440-1770.2006.00309.x

Onyando J. O., Kisoyan P. & Chemelil M. C. (2005) Estimation of Potential Soil Erosion for River Perkerra Catchment in Kenya. *Water Resources Management Journal. 19, 133 – 43.*

Ouyang D, Bartholic J (1997): Predicting sediment delivery ratio in Saginaw Bay watershed. In: Proceedings of the 22nd National Association of Environmental Professionals Conference, 19—23 May 1997, Orlando, FL, pp 659—671.

Ravi, S., Breshears, D. D., Huxman, T. E., & D'Odorico, P. (2010). Land degradation in drylands: interactions among hydrologic–aeolian erosion and vegetation dynamics. Geomorphology, 116(3-4), 236-245.

Refsgaard, J. C., Storm, B., & Clausen, T. (2010). Système Hydrologique Europeén (SHE): review and perspectives after 30 years development in distributed physically-based hydrological modelling. Hydrology Research, 41(5), 355.

Ritchie JC, Nearing MA, Ritchie CA (2003) Patterns of soil erosion and redeposition on lucky hills watershed, walnut gulch experimental watershed, Arizona. 61(2–3):122–130. https://doi.org/10.1016/j.catena.2005.03.012

Rushema, E., Maniragaba, A., Ndihokubwayo, L., & Kulimushi, L. C. (2020). The Impact of Land Degradation on Agricultural Productivity in Nyabihu District-Rwanda, A Case Study of Rugera Sector. IJOEAR, 6(7), 49-63.

Saatsaz, M. (2020). A historical investigation on water resources management in Iran. Environment, Development and Sustainability, 22(3), 1749-1785.

Scherr, S. J. (2003). Developing Countries: An Evaluation of Regional Experience. Land Quality, Agricultural Productivity, and Food Security: Biophysical Processes and Economic Choices at Local, Regional, and Global Levels, 223.

Schertz, D. L. (1983). The basis for soil loss tolerances. Journal of Soil and Water Conservation, 38(1), 10-14.

Scholes, R. J. (2020). The future of semi-arid regions: A weak fabric unravels. Climate, 8(3), 43.

Senut, B., Pickford, M., Gommery, D., Mein, P., Cheboi, K., & Coppens, Y. (2001). First hominid from the Miocene (Lukeino formation, Kenya). Comptes Rendus de l'Académie des Sciences-Series IIA-Earth and Planetary Science, 332(2), 137-144.

Shanshan, W., Baoyang, S., Chaodong, L., Zhanbin, L., & Bo, M. (2018). Runoff and soil erosion on slope Cropland: A Review. *Journal of Resources and Ecology, 9(5), 461-470.*

Simons, D. B., & Şentürk, F. (1992). Sediment transport technology: water and sediment dynamics. Water Resources Publication.

Southgate, D., & Disinger, J. F. (2019). Sustainable resource development in the third world. Routledge.

Srivastava, A., & Chinnasamy, P. (2021). Water management using traditional tank cascade systems: a case study of semi-arid region of Southern India. SN Applied Sciences, 3(3), 1-23.

Stolte, J., Tesfai, M., Øygarden, L., Kværnø, S., Keizer, J., Verheijen, F., ... & Hessel, R. (Eds.). (2015). Soil threats in Europe. Luxembourg: Publications Office.

Sun, L., Zhou, J. L., Cai, Q., Liu, S., & Xiao, J. (2021). Comparing surface erosion processes in four soils from the Loess Plateau under extreme rainfall events. International Soil and Water Conservation Research.

Terer, J. K. (2005). The Study of Hydrologic Characteristics and Management Practices in Agricultural River (Doctoral dissertation, Moi University).

Thomas, J., Joseph, S., & Thrivikramji, K. P. (2018). Assessment of soil erosion in a tropical mountain river basin of the southern Western Ghats, India using RUSLE and GIS. Geoscience Frontiers, 9(3), 893-906.

Tian, P., Gong, Y., Hao, F., Chen, L., Yang, Y., Guo, W., ... & Zhang, W. (2022). Comparing erosion and rill development processes by simulated upslope inflow in two red soils from subtropical China. Catena, 213, 106139.

Tran, D. Q. (2016). Entropy Approach: An Application to Estimation of the Dynamics of Tillage Choice in Iowa (Doctoral dissertation, North Carolina Agricultural and Technical State University).

Tsegaye, L., & Bharti, R. (2021). Soil erosion and sediment yield assessment using RUSLE and GIS-based approach in Anjeb watershed, Northwest Ethiopia. SN Applied Sciences, 3(5), 1-19.

Usharani, K. V., Naik, D., & Manjunatha, R. L. (2019). Pongamia pinnata (L.): composition and advantages in agriculture: a review. J Pharmacogn Phytochem, 8(3), 2181-2187.

Vaezi, A. R., Zarrinabadi, E., & Auerswald, K. (2017). Interaction of land use, slope gradient and rain sequence on runoff and soil loss from weakly aggregated semi-arid soils. Soil and Tillage Research, 172, 22-31.

Vanwalleghem, T., Gómez, J. A., Amate, J. I., De Molina, M. G., Vanderlinden, K., Guzmán, G., ... & Giráldez, J. V. (2017). Impact of historical land use and soil management change on soil erosion and agricultural sustainability during the Anthropocene. Anthropocene, 17, 13-29.

Wairegi, L., van Asten, P., Giller, K. E., & Fairhurst, T. (2016). Banana-coffee system cropping guide.

Wamithi, K. R. (2018). Land use Changes and their Impacts on Wetlands in Loboi Plains Baringo County, Kenya (Doctoral dissertation).

Wang, J., Feng, S., Ni, S., Wen, H., Cai, C., & Guo, Z. (2019). Soil detachment by overland flow on hillslopes with permanent gullies in the Granite area of southeast China. Catena, 183, 104235.

Yang, Y., Weng, B., Man, Z., Yu, Z., & Zhao, J. (2020). Analyzing the contributions of climate change and human activities on runoff in the Northeast Tibet Plateau. Journal of Hydrology: Regional Studies, 27, 100639.

Young, J., Watt, A., Nowicki, P., Alard, D., Clitherow, J., Henle, K., ... & Richards, C. (2005). Towards sustainable land use: identifying and managing the conflicts between human activities and biodiversity conservation in Europe. Biodiversity & Conservation, 14(7), 1641-1661.

Yuan, L., Sinshaw, T., & Forshay, K. J. (2020). Review of watershed-scale water quality and nonpoint source pollution models. Geosciences, 10(1), 25.

Zhang, Y., & Hartemink, A. E. (2017). Sampling designs for soil organic carbon stock assessment of soil profiles. Geoderma, 307, 220-230.

Zhong, J., Peter, W. T., & Wei, Y. (2017). An intelligent and improved density and distance-based clustering approach for industrial survey data classification. Expert Systems with Applications, 68, 21-28.

APPENDICES

Appendix I: Location of Tugen Hills (Google Maps)

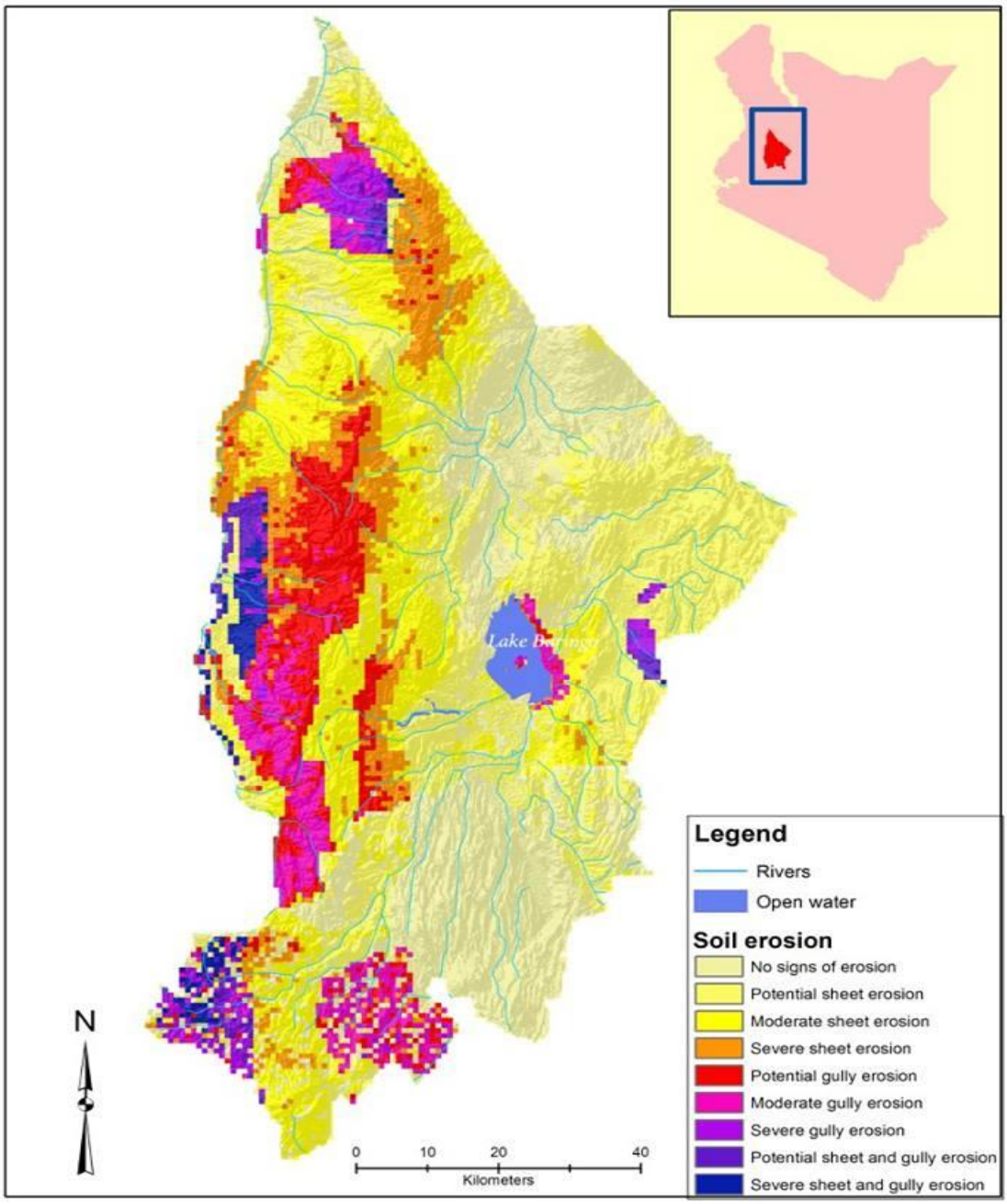

Appendix II: A Complete runoff Plot

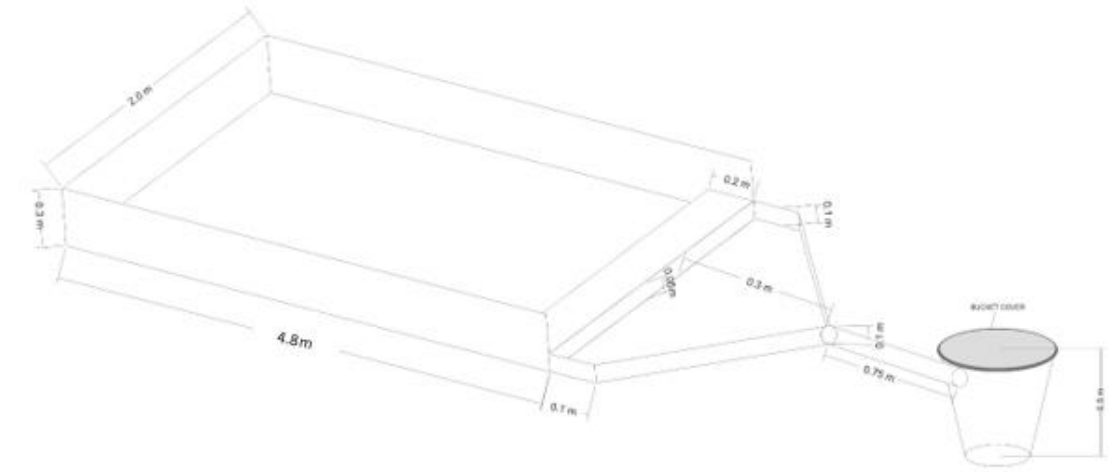

Boundary sheet (Length) folded 90^0 on one end

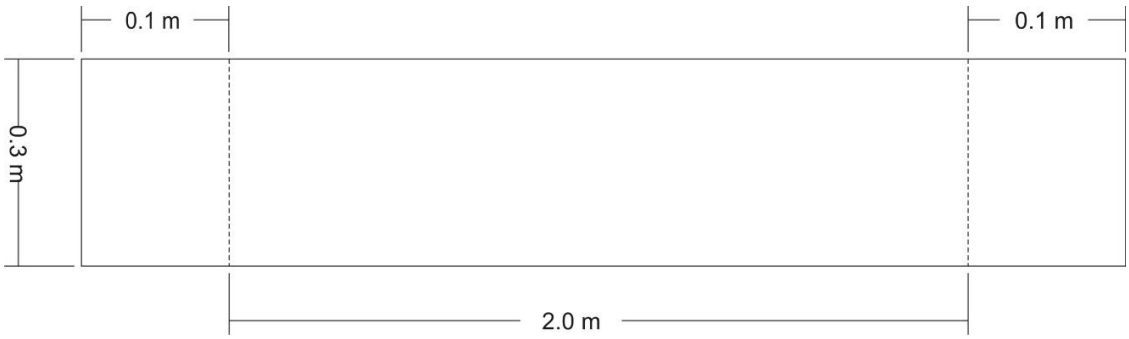

Boundary sheet (width) folded 90^0 on both ends

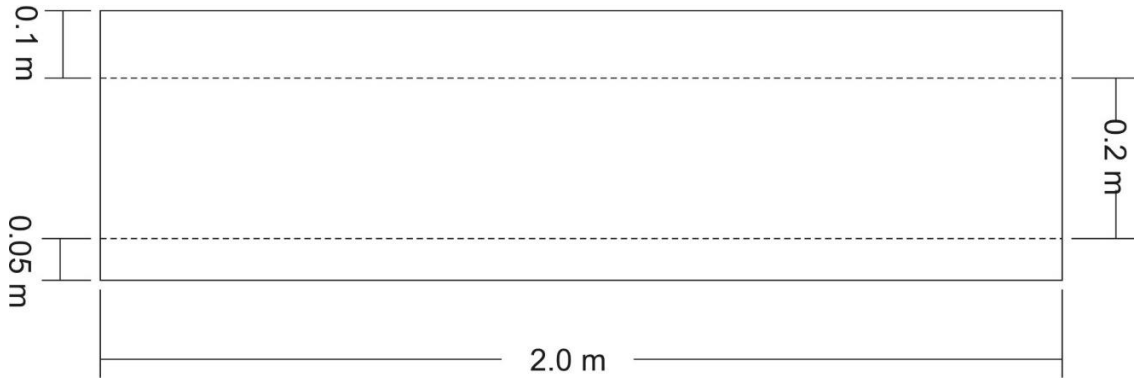

Apron folded 90^0 on both sides

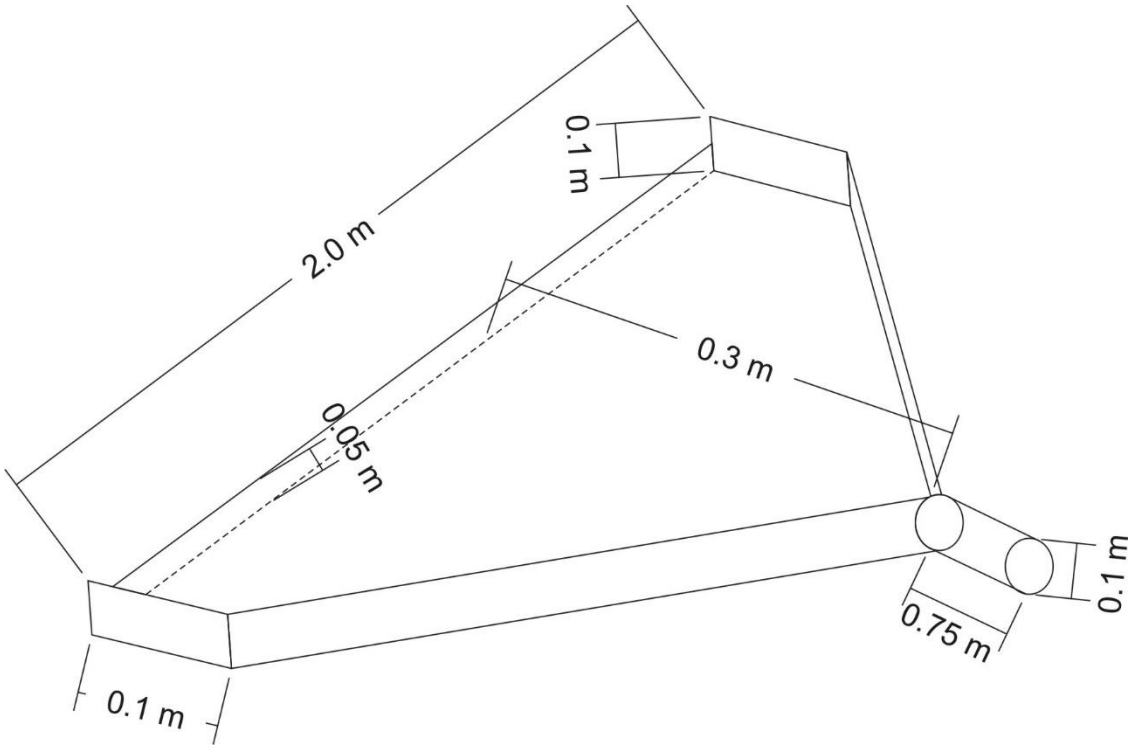

Runoff collector connected with pipe

Appendix III: Run-off Coefficient Tables

	Runoff Coefficient, C					
	Soil Group A			Soil Group B		
Slope :	< 2%	2-6%	> 6%	< 2%	2-6%	> 6%
Forest	0.08	0.11	0.14	0.10	0.14	0.18
Meadow	0.14	0.22	0.30	0.20	0.28	0.37
Pasture	0.15	0.25	0.37	0.23	0.34	0.45
Farmland	0.14	0.18	0.22	0.16	0.21	0.28
Res. 1 acre	0.22	0.26	0.29	0.24	0.28	0.34
Res. 1/2 acre	0.25	0.29	0.32	0.28	0.32	0.36
Res. 1/3 acre	0.28	0.32	0.35	0.30	0.35	0.39
Res. 1/4 acre	0.30	0.34	0.37	0.33	0.37	0.42
Res. 1/8 acre	0.33	0.37	0.40	0.35	0.39	0.44
Industrial	0.85	0.85	0.86	0.85	0.86	0.86
Commercial	0.88	0.88	0.89	0.89	0.89	0.89
Streets: ROW	0.76	0.77	0.79	0.80	0.82	0.84
Parking	0.95	0.96	0.97	0.95	0.96	0.97
Disturbed Area	0.65	0.67	0.69	0.66	0.68	0.70

Rational Method Runoff Coefficients - Part I

Table 0.1: Values of Runoff Coefficient (C) for Rational Formula

Land Use	C	Land Use	C
Business:		***Lawns:***	
		Sandy soil, flat, 2%	0.05 - 0.10
		Sandy soil, avg., 2-7%	0.10 - 0.15
Downtown areas	0.70 - 0.95	Sandy soil, steep, 7%	0.15 - 0.20
Neighborhood areas	0.50 - 0.70	Heavy soil, flat, 2%	0.13 - 0.17
		Heavy soil, avg., 2-7%	0.18 - 0.22
		Heavy soil, steep, 7%	0.25 - 0.35
Residential:		***Agricultural land:***	
		Bare packed soil	
		❖ Smooth	0.30 - 0.60
		❖ Rough	0.20 - 0.50
		Cultivated rows	
Single-family areas	0.30 - 0.50	❖ Heavy soil, no crop	0.30 - 0.60
Multi units, detached	0.40 - 0.60	❖ Heavy soil, with crop	0.20 - 0.50
Munti units, attached	0.60 - 0.75	❖ Sandy soil, no crop	0.20 - 0.40
Suburban	0.25 - 0.40	❖ Sandy soil, with crop	0.10 - 0.25
		Pasture	
		❖ Heavy soil	0.15 - 0.45
		❖ Sandy soil	0.05 - 0.25
		❖ Woodlands	0.05 - 0.25
Industrial:		*Streets:*	
		Asphaltic	0.70 - 0.95
Light areas	0.50 - 0.80	Concrete	0.80 - 0.95
Heavy areas	0.60 - 0.90	Brick	0.70 - 0.85
Parks, cemeteries	0.10 - 0.25	Unimproved areas	0.10 - 0.30
Playgrounds	0.20 - 0.35	Drives and walks	0.75 - 0.85
Railroad yard areas	0.20 - 0.40	Roofs	0.75 - 0.95

Appendix IV: Experimental Data

Table 0.2: Sieve Analysis

Field Ref.	Sieve No.	Log (Sieve No.)	Sieve wt.	Sieve + Sample	Wt. Retained	% retained on each Sieve	Cumulative Percentages	%Finer
		Log (A)			**(D - C)**		**(Total F - F)**	
PT1 1 (250g)	4	0.60205999	554.11	695.15	141.04	56.41	56.41	43.59
	2	0.30103	467.03	511.21	44.18	17.67	74.08	25.92
	1	0	508.98	547.63	38.65	15.46	89.54	10.46
	0.5	-0.30103	497.58	515.44	17.86	7.14	96.68	3.32
	0.25	-0.60206	454.23	459.36	5.13	2.05	98.73	1.27
	0.125	-0.90309	442.32	444.18	1.86	0.74	99.48	0.52
	0.063	-1.2006595	436.59	437.46	0.87	0.35	99.82	0.18
	Pan		406.84	407.28	0.44	0.18	100.00	
	Total				**250.03**			
PT1 2 (270g)	4	0.60205999	554.11	659.34	105.23	42.35	42.35	57.65
	2	0.30103	467.03	520.77	53.74	21.63	63.98	36.02
	1	0	508.98	550.48	41.5	16.70	80.68	19.32
	0.5	-0.30103	497.58	527.28	29.7	11.95	92.63	7.37
	0.25	-0.60206	454.23	466.52	12.29	4.95	97.58	2.42
	0.125	-0.90309	442.32	446.36	4.04	1.63	99.20	0.80
	0.063	-1.2006595	436.59	437.97	1.38	0.56	99.76	0.24
	Pan		406.84	407.44	0.6	0.24	100.00	
	Total				**248.48**			
PT2 1 (271g)	4	0.60205999	554.11	674.78	120.67	48.23	48.23	51.77
	2	0.30103	467.03	509.04	42.01	16.79	65.02	34.98
	1	0	508.98	548.04	39.06	15.61	80.63	19.37
	0.5	-0.30103	497.58	526.32	28.74	11.49	92.12	7.88
	0.25	-0.60206	454.23	466.87	12.64	5.05	97.17	2.83
	0.125	-0.90309	442.32	446.75	4.43	1.77	98.94	1.06
	0.063	-1.2006595	436.59	438.2	1.61	0.64	99.59	0.41
	Pan		406.84	407.87	1.03	0.41	100.00	
	Total				**250.19**			
PT2 2 (277g)	4	0.60205999	554.11	678.32	124.21	49.89	49.89	50.11
	2	0.30103	467.03	500.27	33.24	13.35	63.25	36.75
	1	0	508.98	543.9	34.92	14.03	77.27	22.73
	0.5	-0.30103	497.58	527.72	30.14	12.11	89.38	10.62
	0.25	-0.60206	454.23	473.34	19.11	7.68	97.06	2.94
	0.125	-0.90309	442.32	448.39	6.07	2.44	99.49	0.51
	0.063	-1.2006595	436.59	437.65	1.06	0.43	99.92	0.08
	Pan		406.84	407.04	0.2	0.08	100.00	
	Total				**248.95**			

PT. 3 1 (277g)	4	0.60205999	554.11	670.6	116.49	42.13	42.13	57.87
	2	0.30103	467.03	511.84	44.81	16.20	58.33	41.67
	1	0	508.98	547.92	38.94	14.08	72.41	27.59
	0.5	-0.30103	497.58	552.23	54.65	19.76	92.18	7.82
	0.25	-0.60206	454.23	467.18	12.95	4.68	96.86	3.14
	0.125	-0.90309	442.32	447.25	4.93	1.78	98.64	1.36
	0.063	-1.2006595	436.59	438.94	2.35	0.85	99.49	0.51
	Pan		406.84	408.24	1.4	0.51	100.00	
	Total				**276.52**			
PT. 3 2 (249g)	4	0.60205999	554.11	692	137.89	55.50	55.50	44.50
	2	0.30103	467.03	510.26	43.23	17.40	72.89	27.11
	1	0	508.98	543.58	34.6	13.93	86.82	13.18
	0.5	-0.30103	497.58	520.93	23.35	9.40	96.22	3.78
	0.25	-0.60206	454.23	461.54	7.31	2.94	99.16	0.84
	0.125	-0.90309	442.32	443.93	1.61	0.65	99.81	0.19
	0.063	-1.2006595	436.59	436.96	0.37	0.15	99.96	0.04
	Pan		406.84	406.95	0.11	0.04	100.00	
	Total				**248.47**			

Table 0.3: Total sediments for each plot (Calibration)

Date	Samples	Total volume(ml)	Total Volume (m3)	Measured Total sediment (g)	Peak flow, Q_p (m^3/s)	Soil erodibility, K-factor	Slope length and steepness, LS-factor	Percent Cover	Support practice P-factor	Simulated Total Sediment (g)
14/7/2019	B1 T1	4890	0.00489	56.55	0.00001748	0.18	0.173	35	1	17.785207
	B1 T2	6300	0.0063	15.75	0.000003496	0.18	0.173	30	1	7.2702912
	B1 T3	11030	0.01103	111.20	0.000027968	0.18	0.173	41	1	41.986322
	B2 T1	10030	0.01003	157.61	0.00001748	0.18	0.173	35	1	26.327316
	B2 T2	13580	0.01358	104.29	0.000003496	0.18	0.173	22	1	8.109173
	B2T3	14210	0.01421	274.21	0.000027968	0.18	0.173	31	1	36.454891
	B3 T1	11400	0.0114	105.59	0.00001748	0.18	0.173	43	1	34.687
	B3 T2	11220	0.01122	201.78	0.000003496	0.18	0.173	40	1	13.284546
	B3 T3	13490	0.01349	301.92	0.000027968	0.18	0.173	32	1.000	36.577519
26/07/2019	B1 T1	220	0.00022	11.04	6.66667E-06	0.18	0.173	51	1	2.8157089
	B1 T2	360	0.00036	9.58	1.33333E-06	0.18	0.173	56	1	1.6801434
	B1 T3	120	0.00012	2.53	1.06667E-05	0.18	0.173	39	1	1.9989497
	B2 T1	340	0.00034	11.46	6.66667E-06	0.18	0.173	33	1	2.3107673
	B2 T2	1400	0.0014	82.28	1.33333E-06	0.18	0.173	39.6	1	2.4940104
	B2T3	980	0.00098	11.95	1.06667E-05	0.18	0.173	47	1	7.5824856
	B3 T1	840	0.00084	14.90	6.66667E-06	0.18	0.173	44	1	5.0485185
	B3 T2	750	0.00075	53.84	1.33333E-06	0.18	0.173	38	1	1.7020966
	B3 T3	1100	0.0011	5.28	1.06667E-05	0.18	0.173	46	1	7.904284

Table 0.4: Total sediments for each plot (Validation)

Date	Sample No.	Total Volume, Q, m^3	Peak Flow, q_p,m3/s	Structure class	Soil erodibility, K-factor	Slope length and steepness, LS-factor	Percent Cover	Support Practice, P-factor	Total sediment (g)	
									Measured	Simulated
06/08/2019	B1 T1	0.00011	1.05E-05	2.81	0.18	0.173	83	1	0.71	4.029026
	B1 T2	0.00039	2.11E-06	2.79	0.18	0.173	76	1	5.23	3.057868
	B1 T3	0	1.69E-05	2.83	0.18	0.173	80	1	2.53	0
	B2 T1	0.00065	1.05E-05	2.93	0.18	0.173	42	1	8.81	5.378009
	B2 T2	0.0011	2.11E-06	3	0.18	0.173	37.5	1	13.98	2.657759
	B2T3	0.00068	1.69E-05	3	0.18	0.173	62.3	1	1.43	10.56839
	B3 T1	0.00039	1.05E-05	2.84	0.18	0.173	60	1	2.03	5.812916
	B3 T2	0.000715	2.11E-06	2.9	0.18	0.173	65	1	7.03	3.641232
	B3 T3	0.00175	1.69E-05	2.9	0.18	0.173	59	1	3.53	16.76957
9/8/2019	B1 T1	0.0025	1.05E-05	2.81	0.18	0.173	85	1	24.21	22.67066
	B1 T2	0.00245	2.1E-06	2.79	0.18	0.173	75	1	33.57	8.216338
	B1 T3	0.00234	1.68E-05	2.83	0.18	0.173	79	1	17.74	26.26869
	B2 T1	0.00236	1.05E-05	2.93	0.18	0.173	55	1	30.96	14.21486
	B2 T2	0.00471	2.1E-06	3	0.18	0.173	50	1		7.826575
	B2T3	0.00605	1.68E-05	3	0.18	0.173	72	1	37.63	40.21522
	B3 T1	0.00251	1.05E-05	2.84	0.18	0.173	62	1	24.28	16.57233
	B3 T2	0.01295	2.1E-06	2.9	0.18	0.173	63	1		17.13058
	B3 T3	0.01231	1.68E-05	2.9	0.18	0.173	57	1	38.41	46.92186
12/08/2019	B1 T1	0.00009	7.07E-06	2.81	0.18	0.173	78	1	0.11	2.72887
	B1 T2	0.00026	1.41E-06	2.79	0.18	0.173	77	1	0.59	1.996643
	B1 T3	0.00008	1.13E-05	2.83	0.18	0.173	76.5	1	0.09	3.243918
	B2 T1	0.00021	7.07E-06	2.93	0.18	0.173	53	1	0.35	2.94496
	B2 T2	0.00043	1.41E-06	3	0.18	0.173	52	1		1.774644
	B2T3	0.00061	1.13E-05	3	0.18	0.173	70	1	0.84	8.999315
	B3 T1	0.00027	7.07E-06	2.84	0.18	0.173	61	1	1.1	3.888
	B3 T2	0.00052	1.41E-06	2.9	0.18	0.173	67	1	11.55	2.53657
	B3 T3	0.00102	1.13E-05	2.9	0.18	0.173	65	1	0.24	11.06446
15/08/2019	B1 T1	0.00009	9E-07	2.81	0.18	0.173	82.2	1	1.13	0.933481
	B1 T2	0.00032	1.8E-07	2.79	0.18	0.173	81.6	1	0.05	0.769275
	B1 T3	0	1.44E-06	2.83	0.18	0.173	80	1	0.04	0
	B2 T1	0	9E-07	2.93	0.18	0.173	57	1	0.35	0
	B2 T2	0.0003	1.8E-07	3	0.18	0.173	56	1	1.07	0.509654
	B2T3	0.0003	1.44E-06	3	0.18	0.173	68	1	0.02	1.948782
	B3 T1	0.00021	9E-07	2.84	0.18	0.173	66	1	0.3	1.190399
	B3 T2	0.0002	1.8E-07	2.9	0.18	0.173	72	1	1.14	0.525139
	B3 T3	0.00071	1.44E-06	2.9	0.18	0.173	72	1	0.11	3.26427
20/08/2019	B1 T1	0.00286	2.09E-05	2.81	0.18	0.173	76	1	17.18	31.79566
	B1 T2	0.00162	4.19E-06	2.79	0.18	0.173	85	1	2.22	10.82817
	B1 T3	0.00049	3.35E-05	2.83	0.18	0.173	90.5	1		18.67771
	B2 T1	0.00173	2.09E-05	2.93	0.18	0.173	69	1	11.09	21.93818
	B2 T2	0.00639	4.19E-06	3	0.18	0.173	65	1		17.51691
	B2T3	0.00275	3.35E-05	3	0.18	0.173	78	1	3.99	41.28556
	B3 T1	0.00278	2.09E-05	2.84	0.18	0.173	73	1	4.77	30.07113
	B3 T2	0.01372	4.19E-06	2.9	0.18	0.173	76	1		31.08492
	B3 T3	0.00694	3.35E-05	2.9	0.18	0.173	80	1	35.6	70.19402
28/08/2019	B1 T1	0.00039	3.52E-06	2.81	0.18	0.173	77	1	0.21	4.100388
	B1 T2	0.00048	7.04E-07	2.79	0.18	0.173	90	1	0.23	2.229336
	B1 T3	0.00008	5.63E-06	2.83	0.18	0.173	95.5	1	0.05	2.767916
	B2 T1	0.00083	3.52E-06	2.93	0.18	0.173	73	1	3.45	5.871545
	B2 T2	0.00083	7.04E-07	3	0.18	0.173	85	1	3.85	2.839297
	B2T3	0.00037	5.63E-06	3	0.18	0.173	81	1	0.44	5.417334
	B3 T1	0.00038	3.52E-06	2.84	0.18	0.173	81	1	3.65	4.252651
	B3 T2	0.00236	7.04E-07	2.9	0.18	0.173	74	1	0.37	4.373377
	B3 T3	0.00023	5.63E-06	2.9	0.18	0.173	91	1	0.49	4.694693
10/09/2019	B1 T1	0.0117	1.99E-05	2.81	0.18	0.173	79.8	1		70.14612
	B1 T2	0.00163	3.99E-06	2.79	0.18	0.173	83.3	1	17.76	10.36652
	B1 T3	0.00081	3.19E-05	2.83	0.18	0.173	89	1	2.41	23.53117
	B2 T1	0.00577	1.99E-05	2.93	0.18	0.173	93	1	21.92	55.57202
	B2 T2	0.0117	3.99E-06	3	0.18	0.173	85	1	58.5	31.03002
	B2T3	0.00503	3.19E-05	3	0.18	0.173	82	1		58.76121
	B3 T1	0.00599	1.99E-05	2.84	0.18	0.173	76	1	16.34	46.35108
	B3 T2	0.01525	3.99E-06	2.9	0.18	0.173	80	1		0
	B3 T3	0.00879	3.19E-05	2.9	0.18	0.173	93	1		0

Appendix V: Similarity Report

(3)

Turnitin Originality Report

SOIL EROSION PREDICTION USING MODIFIED UNIVERSAL SOIL LOSS EQUATION (MUSLE) IN TUGEN HILLS, BARINGO, KENYA by Athanus Chesire

From Theses (Theses)

- Processed on 14-Nov-2022 10:48 EAT
- ID: 1953430463
- Word Count: 18638

Similarity Index
38%
Similarity by Source

Internet Sources:
34%
Publications:
17%
Student Papers:
11%

sources:

1 12% match (Internet from 24-Jun-2022)
http://erepository.uoeld.ac.ke/bitstream/handle/123456789/1638/Chesire%20et%20al.%202022.pdf?isAllowed=y&sequence=1

2 2% match (Internet from 28-Mar-2015)
http://scholar.lib.vt.edu/theses/available/etd-04102008-111028/unrestricted/Al-SmadiDissertationV02.pdf

3 2% match (Internet from 18-Oct-2018)
https://docplayer.net/21139013-Soil-management-and-tillage.html

4 1% match (Internet from 29-Oct-2019)
https://www.hydrol-earth-syst-sci-discuss.net/hess-2019-327/hess-2019-327.pdf

5 1% match (Internet from 09-Nov-2022)
https://researchspace.ukzn.ac.za/bitstream/handle/10413/12766/Kollongei_Kipkemboi_Julius_2015.pdf?isAllowed=y&sequence=1

6 1% match (Internet from 26-Sep-2021)
http://ir.iswc.ac.cn/bitstream/361005/7308/2/238---s2.0-S0341816213003093-main.pdf

7 1% match (Internet from 29-Feb-2020)
https://repository.tudelft.nl/islandora/object/uuid:2dd47056-e66a-4de3-bc86-8af4659a74d2/datastream/OBJ/download